

Forward two-photon exchange in elastic lepton-proton scattering and hyperfine splitting correction

Oleksandr Tomalak¹

¹*Institut für Kernphysik and PRISMA Cluster of Excellence,
Johannes Gutenberg Universität, Mainz, Germany*

(Dated: February 27, 2017)

We relate the forward two-photon exchange (TPE) amplitudes to integrals of the inclusive cross sections. These relations yield an alternative way for the evaluation of the TPE correction to hyperfine-splitting (HFS) in the hydrogen-like atoms with an equivalent to the standard approach (Iddings, Drell and Sullivan) result implying the Burkhardt-Cottingham sum rule. For evaluation of the individual effects (e.g., elastic contribution) our approach yields the distinct result. We reevaluate the Zemach, recoil and polarizability corrections expressing them through the low-energy proton structure constants. The uncertainty of the TPE correction to S energy levels in muonic hydrogen of 98 ppm exceeds the ppm accuracy level of the forthcoming 1S HFS measurements at PSI, J-PARC and RIKEN-RAL.

Contents

I. Introduction	2
II. Forward lepton-proton scattering	4
III. Relation of the forward two-photon amplitudes to the proton structure	7
IV. Lamb shift and hyperfine splitting (HFS)	10
A. Resulting HFS correction evaluation	12
B. Zemach correction evaluation	16
C. Polarizability correction evaluation	17
V. Conclusions and outlook	21
VI. Acknowledgments	22
A. Crossing in lepton-proton scattering	22
B. Dispersion relations verification in QED	23
C. Forward invariant amplitudes in terms of the proton structure functions	25
D. HFS through the forward double virtual Compton scattering amplitudes	26
E. Forward scattering observables	28
References	30

I. INTRODUCTION

The two-photon exchange (TPE) corrections could be responsible for the discrepancy in the ratio of the proton electric to magnetic form factors between the traditional Rosenbluth separation [1] and the polarization transfer [2] methods, cf. [3, 4] and [5, 6] for reviews. These corrections introduce the largest hadronic uncertainty in the elastic electron-proton scattering experiments and should be precisely accounted for in analysis of the modern data. Dedicated experiments to measure the TPE correction from the ratio of the elastic electron-proton to positron-proton scattering cross sections, where TPE enters with different signs, have recently been carried out at VEPP-3 (Novosibirsk) [7], OLYMPUS (DESY) [8], and CLAS (JLab) [9]. These measurements show an evidence of a significant TPE effect.

The TPE effects also play a prominent role in evaluation of the proton structure (finite size) contributions to the spectrum of hydrogen (H) and muonic hydrogen (μH). The uncertainty of TPE is the dominant uncertainty in the precise spectroscopy measurements with the muonic hydrogen. These corrections received a renewed attention in light of the so-called *proton radius puzzle*, the discrepancy in the extracted proton charge radius from the muonic hydrogen Lamb shift [10, 11] and measurements with electrons [12–14], see [11, 15] for recent reviews. One of the recent achievements in this field is the measurement of the 2S hyperfine splitting (HFS) in muonic hydrogen by the CREMA Collaboration at PSI [11]. Also a high-precision measurement of 1S HFS in muonic hydrogen with an unprecedented ppm accuracy level is planned by this [16, 17] and other collaborations [18, 19]. Such accurate measurements will strictly constrain the elastic and inelastic proton structure.

To evaluate the contribution from the diagrams with two exchanged photons to atomic spectrum one notices that the lower part of the TPE graph, see Fig. 1, corresponds with the process of forward doubly virtual Compton scattering (VVCS). The latter in the forward kinematics can be expressed through dispersion relations (DRs) in terms of the proton structure functions (SFs) measured in elastic and inelastic electron-proton (ep) scattering. The forward TPE is thus evaluated, performing the Wick rotation, as an integral over the photon energy, ν_γ , and virtuality, $Q^2 > 0$. For the Lamb shift correction evaluation [20–25] the subtraction function is needed in addition. However, the latter can be estimated at low virtualities from the chiral perturbation theory [26–28] or non-relativistic quantum electrodynamics (NRQED) [29] and at high virtualities from the operator product expansion [30]. This function, in principle, can be also determined with account of the high-energy SFs data [31–33]. The leading TPE effects of the proton structure in HFS can be entirely expressed in terms of SFs [34–43]. Consequently, the dominant uncertainty from the TPE correction can be reduced by the precise measurements of the proton electric and magnetic form factors in the low- Q^2 region [44] and measurements of the proton spin structure functions g_1 and g_2 by EG4, SANE and g2p experiments at JLab [45–47]. For recent numerical evaluations of the TPE correction to HFS see Refs. [41–43], for the evaluation within framework of NRQED see Ref. [48] and for results in chiral EFT see Ref. [49].

In this work we provide a different way to express the forward TPE contributions in terms of the proton SFs. We are working on the level of the forward lepton-proton scattering amplitudes and account for the forward double spin-flip amplitude (i.e., the one where the helicities of both lepton and proton are flipped) for the first time. The method we are using to derive these relations is akin to deriving sum rules for Compton or light-by-light scattering [50, 51]. For the scattering of two charged particles the derivation changes quite a bit. The crossing relates the amplitude of the particle scattering with the amplitude of

the antiparticle scattering [52, 53]. Nevertheless, for the TPE amplitudes we exploit the crossing in one channel due to the charge independence of the TPE contributions. In this way our dispersion relations (DRs) for the elastic lepton-proton scattering do not involve the crossed channels, and hence are different from generic DRs for charged particles, such as the DRs for the nucleon-nucleon scattering [52–54]. Advantageously, the method based on DRs for lp amplitudes [55–57] has no complications due to the poles contributions arising after the Wick rotation when one considers amplitudes above the threshold.

We express the TPE corrections to the Lamb shift and HFS of S energy levels through the forward TPE amplitudes at threshold. With DRs for the lepton-proton amplitudes we are not able to express the correction to the Lamb shift through the experimental information, but the correction to the hyperfine splitting is entirely expressed through the proton spin SFs. The resulting HFS correction agrees with the standard approach of Iddings, Drell and Sullivan *et al.* [35–40] only after account for the Burkhardt-Cottingham (BC) sum rule. However, the contribution of each individual channel to the TPE correction in this work differs from the literature result. Afterwards, we reevaluate the TPE correction to HFS in H and μ H exploiting the DRs for the lepton-proton amplitudes and for the VVCS amplitudes. We connect the region with small photons virtualities in HFS integrand that we express in terms of moments of the spin SFs to the region with large photons virtualities, where both methods give the same results. We also reevaluate the Zemach, recoil and polarizability corrections and corresponding uncertainties accounting for the MAMI data on the elastic proton form factors [12, 13]. We express the polarizability correction in terms of the measurable spin asymmetry, which provides a direct relation of this correction to the experimental observables.

The paper is organized as follows. We write down DRs for the forward elastic lp scattering TPE amplitudes in terms of the inclusive lp cross sections at leading α order in Sec. II and verify them in QED in App. B. We relate the inclusive lp cross sections and the forward TPE amplitudes to proton SFs in Sec. III. Subsequently, we derive the leading proton structure corrections coming from TPE to the hydrogen and muonic hydrogen S energy levels and present the results of the numerical evaluation of the proton and inelastic intermediate states TPE contributions to HFS in Sec. IV. We give our conclusions with outlook of the forthcoming 1S HFS measurements in Sec. V. We also provide the derivation of the TPE correction to HFS using the forward Compton scattering tensor in App. D. In App. E we classify all possible elastic scattering polarization observables in the forward kinematics.

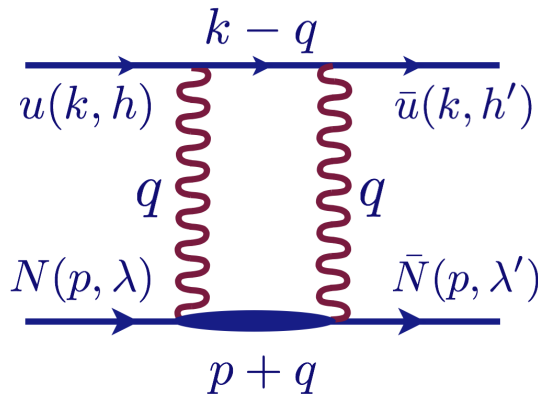


FIG. 1: Two-photon exchange graph.

II. FORWARD LEPTON-PROTON SCATTERING

The forward elastic lp scattering is described by three non-vanishing independent helicity amplitudes $T_{h'\lambda'h\lambda}$, with h (h') and λ (λ') the helicities of the initial (final) lepton and proton, see Fig. 1 for the notations of kinematics and helicities:

$$T_{++++}, \quad T_{+--+}, \quad T_{--++}, \quad (1)$$

which are functions of the lepton energy ω in the lab frame. We denote the positive helicity as $+$ and the negative helicity as $-$. The contribution with exchange of a fixed number of photons to the following three amplitudes has definite even-odd properties with respect to the crossing $\omega \rightarrow -\omega$:

$$f_{\pm}(\omega) = \frac{1}{2}(T_{++++} \pm T_{+--+}), \quad (2a)$$

$$g(\omega) = \frac{1}{2}T_{--++}. \quad (2b)$$

The Lorentz structure of the forward amplitude is then given by

$$\begin{aligned} T_{h'\lambda'h\lambda}(\omega) &= \frac{f_+(\omega)}{4mM} \bar{u}(k, h') u(k, h) \bar{N}(p, \lambda') N(p, \lambda) \\ &\quad - \frac{mf_-(\omega) + \omega g(\omega)}{8M\vec{k}^2} \bar{u}(k, h') \gamma^{\mu\nu} u(k, h) \bar{N}(p, \lambda') \gamma_{\mu\nu} N(p, \lambda) \\ &\quad + \frac{\omega f_-(\omega) + mg(\omega)}{4M\vec{k}^2} \bar{u}(k, h') \gamma_{\mu} \gamma_5 u(k, h) \bar{N}(p, \lambda') \gamma^{\mu} \gamma_5 N(p, \lambda), \end{aligned} \quad (3)$$

with m and u the lepton mass and spinor, \vec{k} the lepton momentum in the lab frame, M and N the proton mass and spinor, $\gamma^{\mu\nu} = \frac{1}{2}[\gamma^{\mu}, \gamma^{\nu}]$, where γ^{μ} are the Dirac matrices, the spinors are normalized as

$$\bar{u}(k, h') u(k, h) = 2m\delta_{h'h}, \quad \bar{N}(p, \lambda') N(p, \lambda) = 2M\delta_{\lambda'\lambda}. \quad (4)$$

In order to establish the even-odd properties for the invariant amplitudes under $\omega \rightarrow -\omega$, we first perform the crossing on the lepton line and relate amplitudes of the lepton-proton scattering $f^{l-p}(\omega)$ in the physical region ($\omega > 0$) to amplitudes of the antilepton-proton scattering $f^{l+p}(-\omega)$ in the unphysical region ($\omega < 0$):

$$f_+^{l+p}(\omega) = f_+^{l-p}(-\omega), \quad (5)$$

$$f_-^{l+p}(\omega) = -f_-^{l-p}(-\omega), \quad (6)$$

$$g^{l+p}(\omega) = g^{l-p}(-\omega), \quad (7)$$

where ω is treated as a complex variable, see Appendix A for details of this derivation. The perturbative contributions with odd number of photons connected to the lepton (antilepton) line have different sign in the amplitudes of the lepton-proton and antilepton-proton scattering as compared to the contributions with an even number of photons, which have the same sign. We express the scattering amplitudes in terms of the contributions with even $f^{(2n)\gamma}(\omega)$ and odd $f^{(2n-1)\gamma}(\omega)$ number of photons connected to the lepton line, e.g.:

$$f_{\pm}^{l\pm p} = \sum_{n=1}^{\infty} \left(f_{\pm}^{(2n)\gamma} \pm f_{\pm}^{(2n-1)\gamma} \right), \quad (8)$$

and obtain the following crossing relations for the contribution of graphs with n exchanged photons on the real ω axis:

$$f_+^{n\gamma}(\omega) = (-1)^n (f_+^{n\gamma}(-\omega))^*, \quad (9)$$

$$f_-^{n\gamma}(\omega) = -(-1)^n (f_-^{n\gamma}(-\omega))^*, \quad (10)$$

$$g^{n\gamma}(\omega) = (-1)^n (g^{n\gamma}(-\omega))^*. \quad (11)$$

As usual, the optical theorem establishes the relations between the imaginary parts of the forward amplitudes and the total inclusive cross sections of lp collisions:

$$\Im f_{\pm}(\omega) = M|\vec{k}|(\sigma_{++}(\omega) \pm \sigma_{+-}(\omega)), \quad (12)$$

$$\Im g(\omega) = 2M|\vec{k}|(\sigma_{\parallel}(\omega) - \sigma_{\perp}(\omega)), \quad (13)$$

where $\sigma_{h\lambda}$ is the inclusive cross section with the incoming lepton helicity h and the incoming proton helicity λ ; σ_{\perp} (σ_{\parallel}) is the inclusive cross section with lepton and proton polarized transversely and perpendicular (parallel) to each other.

The elastic (proton) contribution to the inclusive cross section is infrared divergent. This divergence should be subtracted in a proper way in all three amplitudes. We realize this subtraction only for the case of amplitudes at threshold in Section IV.

We express the latter cross sections in terms of the proton SFs up to the order α^2 in Section III and obtain the imaginary parts of the TPE amplitudes at the leading α order with Eqs. (12-13).

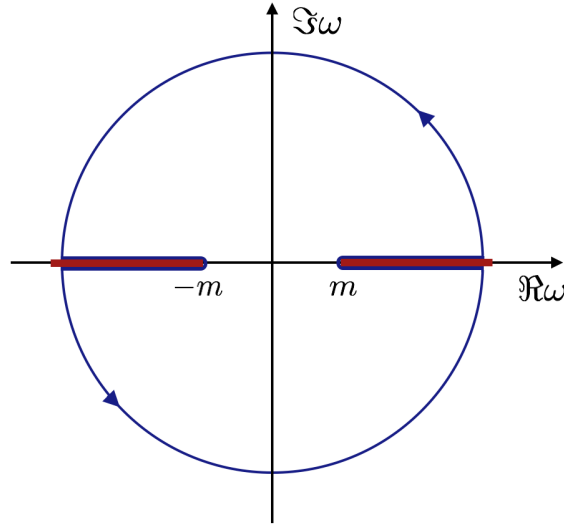


FIG. 2: Complex plane of the ω variable.

Assuming analyticity of these amplitudes in the entire complex ω -plane, except for the branch cuts along the real axis extending from threshold to infinity, see Fig. 2, we can write down the standard DRs:

$$\Re \left\{ \begin{matrix} f_{\pm}(\omega) \\ g(\omega) \end{matrix} \right\} = \frac{1}{\pi} \left(\overset{-m}{\underset{-\infty}{\int}} + \overset{\infty}{\underset{m}{\int}} \right) \frac{d\omega'}{\omega' - \omega} \Im \left\{ \begin{matrix} f_{\pm}(\omega') \\ g(\omega') \end{matrix} \right\}, \quad (14)$$

where \oint stands for the principal-value integration. Using properties of the TPE amplitudes under the crossing $\omega \rightarrow -\omega$, see Eqs. (9-11), we write down DRs valid at the leading α order and thereby account for both direct and crossed graphs:

$$\Re f_+^{2\gamma}(\omega) = \frac{4M}{\pi} \oint_m^\infty \frac{\omega' |\vec{k}'| \sigma(\omega')}{\omega'^2 - \omega^2} d\omega', \quad (15)$$

$$\Re f_-^{2\gamma}(\omega) = \frac{2M\omega}{\pi} \oint_m^\infty \frac{|\vec{k}'| (\sigma_{++}(\omega') - \sigma_{+-}(\omega'))}{\omega'^2 - \omega^2} d\omega', \quad (16)$$

$$\Re g^{2\gamma}(\omega) = \frac{4M}{\pi} \oint_m^\infty \frac{\omega' |\vec{k}'| (\sigma_{\parallel}(\omega') - \sigma_{\perp}(\omega'))}{\omega'^2 - \omega^2} d\omega', \quad (17)$$

with the lepton momentum in the lab frame $|\vec{k}'| = \sqrt{\omega'^2 - m^2}$. These DRs are written for amplitudes in one channel contrary to the DRs for the forward proton-proton scattering [52].

The high-energy behavior of the total unpolarized inclusive cross section requires a subtraction in the DR for the amplitude $f_+^{2\gamma}$, e.g., at the point ω_s :¹

$$\Re f_+^{2\gamma}(\omega) - \Re f_+^{2\gamma}(\omega_s) = \frac{4M(\omega^2 - \omega_s^2)}{\pi} \oint_m^\infty \frac{\omega' |\vec{k}'| \sigma(\omega')}{(\omega'^2 - \omega^2)(\omega'^2 - \omega_s^2)} d\omega'. \quad (18)$$

The lepton-proton DRs were checked at the leading QED order, see Appendix B for details. However the Regge behavior of the proton SF F_1 makes the inclusive cross section σ divergent due to the virtual photons with high energy in the lab frame. Consequently the DR cannot be written for the inelastic TPE contribution to the unpolarized amplitude f_+ .

The DRs of Eqs. (16-18) have the same form as the DRs for the light-by-light scattering [51].

We decompose the forward scattering amplitudes into a sum of one-photon exchange (OPE) and TPE contributions. The TPE amplitudes, except for $\Re f_+^{2\gamma}$, are obtained with DRs and unitarity relations as described above. The OPE amplitudes are real and given by

$$f_-^{1\gamma} = e^2 \mu_P, \quad (19)$$

$$g^{1\gamma} = 0, \quad (20)$$

with the proton magnetic moment $\mu_P \approx 2.793$. The vacuum polarization correction is zero in the forward scattering. The lepton vertex correction does not change the amplitude g , modifies the amplitude f_- by the lepton anomalous magnetic moment a_l : $\delta f_- = a_l e^2$ and contributes to the amplitude f_+ . The proton vertex correction with the proton intermediate state contributes to f_- and f_+ amplitudes [59]. The contribution of inelastic intermediate states is expected to be small. However, this correction requires an additional theoretical investigation. Therefore, the forward amplitudes are completely expressed in terms of the total inclusive cross sections, see Eqs. (12, 13, 16, 17), at $O(\alpha^2)$ up to the one unknown spin-independent amplitude $\Re f_+$.

¹ In the language of effective field theories this subtraction corresponds to the counter term, which was studied in context of the atomic physics and muon-proton scattering in Ref. [58].

III. RELATION OF THE FORWARD TWO-PHOTON AMPLITUDES TO THE PROTON STRUCTURE

In this Section, we first express the total inclusive cross sections in terms of the experimentally measured proton SFs. Exploiting these relations, we express the real parts of the forward TPE amplitudes as integrals over the photon energy ν_γ in the lab frame and photon virtuality Q^2 .

A common way to express the differential inelastic e^-p scattering cross section assumes the exchange of one photon. The cross section is given by the contraction of the leptonic tensor $L^{\mu\nu}$ and the hadronic tensor $W^{\mu\nu}$ [60]. It is proportional to the phase space of the final lepton (with 4-momentum $k' = (\omega', \vec{k}')$ in the lab frame) and given by

$$d\sigma = \frac{e^4}{4M\sqrt{\omega^2 - m^2}} \frac{d^3\vec{k}'}{(2\pi)^3 2\omega'} (4\pi) L^{\mu\nu} W_{\mu\nu}, \quad (21)$$

with the unit of electric charge e . The kinematics are traditionally described by the kinematical Bjorken variable x_{Bj} , the variable y related to the energy transferred by the virtual photon relative to the beam energy and the momentum transfer Q^2 :

$$x_{\text{Bj}} = \frac{Q^2}{2(p \cdot q)}, \quad y = \frac{(p \cdot q)}{(p \cdot k)} = \frac{Q^2}{2x_{\text{Bj}} M \omega}, \quad Q^2 = -q^2 = -(k - k')^2. \quad (22)$$

The leptonic tensor is evaluated in QED. It is given by

$$L^{\mu\nu} = 2 (k^\mu k'^\nu + k'^\mu k^\nu + (m^2 - (k \cdot k')) g^{\mu\nu} - i m \varepsilon^{\mu\nu\rho\sigma} q_\rho s_\sigma), \quad (23)$$

where s^μ is the lepton spin vector: $s^\mu s_\mu = -1$, $(s \cdot k) = 0$. The general Lorentz and gauge invariant structure of the hadronic tensor $W^{\mu\nu}$ which preserves parity and charge conjugation invariance is given by

$$W_{\mu\nu} = \left(-g_{\mu\nu} + \frac{q_\mu q_\nu}{q^2} \right) F_1(\nu_\gamma, Q^2) + \frac{1}{(p \cdot q)} \left(p^\mu - \frac{p \cdot q}{q^2} q^\mu \right) \left(p^\nu - \frac{p \cdot q}{q^2} q^\nu \right) F_2(\nu_\gamma, Q^2) \\ + i \varepsilon_{\mu\nu\alpha\beta} \frac{M q^\alpha}{(p \cdot q)} \left[S^\beta g_1(\nu_\gamma, Q^2) + \left(S^\beta - \frac{(S \cdot q)}{(p \cdot q)} p^\beta \right) g_2(\nu_\gamma, Q^2) \right], \quad (24)$$

with the virtual photon energy in the laboratory frame $\nu_\gamma = (p \cdot q)/M$ and the proton SFs $F_1(\nu_\gamma, Q^2)$, $F_2(\nu_\gamma, Q^2)$, $g_1(\nu_\gamma, Q^2)$, $g_2(\nu_\gamma, Q^2)$, which are extracted from the experimental data. The proton spin 4-vector satisfies: $S^2 = -1$, $(S \cdot p) = 0$.

The total unpolarized cross section is given by

$$\frac{d^2\sigma}{d\nu_\gamma dQ^2} = \frac{\pi\alpha^2}{(Q^2)^2} \frac{2}{\omega^2 - m^2} \left(\frac{Q^2 - 2m^2}{M} F_1(\nu_\gamma, Q^2) + \left(\frac{2\omega^2}{\nu_\gamma} - 2\omega - \frac{Q^2}{2\nu_\gamma} \right) F_2(\nu_\gamma, Q^2) \right). \quad (25)$$

This expression reduces to the known expression [60] in the massless limit.

Consider a scattering of longitudinally polarized leptons on the proton polarized in the lepton momentum direction $\sigma_{h\lambda} = \sigma_{+-}$ and the scattering on the proton polarized in the

opposite direction $\sigma_{h\lambda} = \sigma_{++}$ with the proton (lepton) spin vector in the laboratory frame $S^\mu = (0, -\lambda \hat{k})$ ($s^\mu = (|\vec{k}|, \omega \hat{k})/m$) and $\hat{k} = \vec{k}/|\vec{k}|$. For the cross sections difference we obtain:

$$\begin{aligned} \frac{d^2\sigma_{++} - d^2\sigma_{+-}}{d\nu_\gamma dQ^2} &= \frac{4\pi\alpha^2}{\nu_\gamma M Q^2} \frac{\omega}{\omega^2 - m^2} \left\{ -\frac{Q^2}{\nu_\gamma \omega} g_2(\nu_\gamma, Q^2) \right. \\ &\quad \left. + \left(2 - \frac{Q^2}{2(\omega^2 - m^2)} \left(1 + \frac{2\nu_\gamma m^2}{Q^2 \omega} \right) \left(1 + \frac{2\nu_\gamma \omega}{Q^2} \right) \right) g_1(\nu_\gamma, Q^2) \right\}. \end{aligned} \quad (26)$$

This expression reduces to the known expression [60], [61] in the massless limit.

Consider the scattering of transversely polarized leptons on transversely polarized protons. Denoting the averaged over the azimuthal angle cross section σ_\perp (σ_\parallel) for scattering with perpendicular (parallel) spin vectors of lepton ($s^\mu = (0, \cos \phi_l, \sin \phi_l, 0)$) and proton ($S^\mu = (0, \cos \phi_p, \sin \phi_p, 0)$),² i. e. $\phi_l - \phi_p = \pm\pi/2$ ($\phi_l - \phi_p = 0$) for the perpendicular (parallel) configuration, we obtain:

$$\begin{aligned} \frac{d^2\sigma_\perp - d^2\sigma_\parallel}{d\nu_\gamma dQ^2} &= \frac{2\pi m \alpha^2}{\nu_\gamma M Q^2} \frac{1}{\omega^2 - m^2} \left\{ 2g_2(\nu_\gamma, Q^2) \right. \\ &\quad \left. + \left(1 + \frac{\omega \nu_\gamma}{\omega^2 - m^2} \left(1 + \frac{m^2 \nu_\gamma}{\omega Q^2} + \frac{Q^2}{4\nu_\gamma \omega} \right) \right) g_1(\nu_\gamma, Q^2) \right\}. \end{aligned} \quad (27)$$

Consequently, a measurement of the inclusive e^-p cross sections accesses the proton spin SFs g_1 and g_2 .

The elastic scattering cross sections $l^-p \rightarrow l^-p$ are obtained by substitution of the inelastic SFs by the elastic contribution to them:

$$F_1^{\text{el}}(x_{\text{Bj}}, Q^2) = \frac{1}{2} G_M^2(Q^2) \delta(1 - x_{\text{Bj}}), \quad (28)$$

$$F_2^{\text{el}}(x_{\text{Bj}}, Q^2) = \frac{G_E^2(Q^2) + \tau_P G_M^2(Q^2)}{1 + \tau_P} \delta(1 - x_{\text{Bj}}), \quad (29)$$

$$g_1^{\text{el}}(x_{\text{Bj}}, Q^2) = \frac{1}{2} F_D(Q^2) G_M(Q^2) \delta(1 - x_{\text{Bj}}), \quad (30)$$

$$g_2^{\text{el}}(x_{\text{Bj}}, Q^2) = -\frac{1}{2} \tau_P F_P(Q^2) G_M(Q^2) \delta(1 - x_{\text{Bj}}), \quad (31)$$

where $F_D(Q^2)$, $F_P(Q^2)$, $G_E(Q^2)$, $G_M(Q^2)$ are the Dirac, Pauli, Sachs electric and magnetic proton form factors and $\tau_P = Q^2/(4M^2)$.

Substituting the expressions for the inclusive cross sections of Eqs. (25-27) into the DRs, see Eqs. (16-17), changing the integration order, as detailed in Appendix C, and expressing the spin-dependent forward TPE amplitudes in terms of the proton SFs, we obtain:

² The nontrivial relation $\sigma_\perp = \sigma$ holds for the lepton-proton scattering. We have obtained this relation in the OPE approximation of Eq. (21) and have proved it by the direct cross sections evaluation for the case of elastic scattering and exploiting the symmetry properties of the helicity amplitudes for the scattering to arbitrary channel $lp \rightarrow lX$.

$$\begin{aligned}
\Re g^{2\gamma}(\omega) = & \frac{4m\alpha^2}{\vec{k}^2} \int_0^\infty \frac{dQ^2}{Q^2} \int_{\nu_{\text{thr}}}^\infty \frac{d\nu_\gamma}{\nu_\gamma} \\
& \left\{ 2 \frac{(\omega_0 - |\vec{k}_0|)\nu_\gamma + m^2(\tau_l + \tilde{\tau})}{|\vec{k}_0|} g_1(\nu_\gamma, Q^2) \right. \\
& + \frac{m^2(\tau_l + \tilde{\tau}) + \vec{k}^2}{|\vec{k}|} g_1(\nu_\gamma, Q^2) \ln \frac{|\vec{k}| - |\vec{k}_0|}{|\vec{k}| + |\vec{k}_0|} + 2g_2(\nu_\gamma, Q^2) \ln \frac{|\vec{k}| - |\vec{k}_0|}{|\vec{k}| + |\vec{k}_0|} \\
& \left. + \frac{\omega\nu_\gamma}{|\vec{k}|} g_1(\nu_\gamma, Q^2) \ln \frac{(\omega + |\vec{k}|)^2 (\omega_0^2 - \omega^2)}{(\omega|\vec{k}_0| + |\vec{k}|\omega_0)^2} \right\}, \tag{32}
\end{aligned}$$

$$\begin{aligned}
\Re f_-^{2\gamma}(\omega) = & \frac{8\omega\alpha^2}{\vec{k}^2} \int_0^\infty \frac{dQ^2}{Q^2} \int_{\nu_{\text{thr}}}^\infty \frac{d\nu_\gamma}{\nu_\gamma} \\
& \left\{ 2 \frac{(\omega_0 - |\vec{k}_0|)\nu_\gamma + m^2(\tau_l + \tilde{\tau})}{|\vec{k}_0|} g_1(\nu_\gamma, Q^2) \right. \\
& + \frac{m^2(\tau_l + \tilde{\tau}) - \vec{k}^2}{|\vec{k}|} g_1(\nu_\gamma, Q^2) \ln \frac{|\vec{k}| - |\vec{k}_0|}{|\vec{k}| + |\vec{k}_0|} \\
& + \frac{Q^2|\vec{k}|}{2\omega\nu_\gamma} g_2(\nu_\gamma, Q^2) \ln \frac{(\omega + |\vec{k}|)^2 (\omega_0^2 - \omega^2)}{(\omega|\vec{k}_0| + |\vec{k}|\omega_0)^2} \\
& \left. + \frac{(\omega^2 + m^2)\nu_\gamma}{2\omega|\vec{k}|} g_1(\nu_\gamma, Q^2) \ln \frac{(\omega + |\vec{k}|)^2 (\omega_0^2 - \omega^2)}{(\omega|\vec{k}_0| + |\vec{k}|\omega_0)^2} \right\}, \tag{33}
\end{aligned}$$

where we have introduced the notations:

$$|\vec{k}| = \sqrt{\omega^2 - m^2}, \quad |\vec{k}_0| = \sqrt{\omega_0^2 - m^2}, \tag{34}$$

$$\omega_0 = m \left(\sqrt{\tau_l \tilde{\tau}} + \sqrt{1 + \tau_l} \sqrt{1 + \tilde{\tau}} \right), \tag{35}$$

$$\tau_l = \frac{Q^2}{4m^2}, \quad \tau_P = \frac{Q^2}{4M^2}, \quad \tilde{\tau} = \frac{\nu_\gamma^2}{Q^2}. \tag{36}$$

In Eqs. (33, 32) the elastic threshold ν_{thr} and the inelastic threshold $\nu_{\text{thr}}^{\text{inel}}$ are given by $\nu_{\text{thr}} = 0$ and $\nu_{\text{thr}}^{\text{inel}} = m_\pi + (m_\pi^2 + Q^2) / (2M)$ respectively, where m_π denotes the pion mass.

The leading TPE correction to the atomic energy levels is given by the values of the amplitudes at threshold $\omega = m$. The TPE amplitudes $f_-^{2\gamma}$, $g^{2\gamma}$ at threshold can then be expressed in terms of the proton spin SFs as

$$f_-^{2\gamma}(m) = \frac{16\alpha^2}{3} \int_0^\infty \frac{dQ^2}{Q^2} \int_{\nu_{\text{thr}}}^\infty \frac{d\nu_\gamma}{\nu_\gamma} \frac{[2 + \rho(\tau_l) \rho(\tilde{\tau})] g_1(\nu_\gamma, Q^2) - 3\rho(\tau_l) \rho(\tilde{\tau}) g_2(\nu_\gamma, Q^2) / \tilde{\tau}}{\sqrt{\tilde{\tau}} \sqrt{1 + \tau_l} + \sqrt{\tau_l} \sqrt{1 + \tilde{\tau}}}, \tag{37}$$

$$g^{2\gamma}(m) = -\frac{16\alpha^2}{3} \int_0^\infty \frac{dQ^2}{Q^2} \int_{\nu_{\text{thr}}}^\infty \frac{d\nu_\gamma}{\nu_\gamma} \frac{[2 + \rho(\tau_l) \rho(\tilde{\tau})] g_1(\nu_\gamma, Q^2) + 3g_2(\nu_\gamma, Q^2)}{\sqrt{\tilde{\tau}}\sqrt{1+\tau_l} + \sqrt{\tau_l}\sqrt{1+\tilde{\tau}}}, \quad (38)$$

with

$$\rho(\tau) = \tau - \sqrt{\tau(1+\tau)}. \quad (39)$$

Evaluating the sum of the spin-dependent lepton-proton TPE amplitudes in the DR approach, see Eqs. (37, 38), we obtain:

$$g^{2\gamma}(m) + f_-^{2\gamma}(m) = 64\alpha^2 Mm \int_0^\infty \frac{dQ^2}{Q^4} \rho(\tau_l) \int_0^1 dx_{\text{Bj}} g_2(x_{\text{Bj}}, Q^2) = 0, \quad (40)$$

which is a trivial relation due to the Burkhardt-Cottingham (BC) sum rule.

IV. LAMB SHIFT AND HYPERFINE SPLITTING (HFS)

In the lp center-of-mass (c.m.) reference frame the TPE forward scattering amplitude $T^{2\gamma}$ is expressed in terms of the forward amplitudes $f_+^{2\gamma}$, $f_-^{2\gamma}$, $g^{2\gamma}$ as

$$T^{2\gamma}(\omega) = f_+^{2\gamma}(\omega) + 4g^{2\gamma}(\omega) \mathbf{s} \cdot \mathbf{S} + 4(f_-^{2\gamma}(\omega) + g^{2\gamma}(\omega)) \mathbf{s} \cdot \hat{\mathbf{k}} \mathbf{S} \cdot \hat{\mathbf{p}}, \quad (41)$$

with \mathbf{s} (\mathbf{S}) and $\hat{\mathbf{k}}$ ($\hat{\mathbf{p}}$) the lepton (proton) spin and momentum direction vectors. This decomposition often arises in the analysis of the non-relativistic forward neutron-proton scattering, see e.g. [54].

It is then easy to see that, considering $T^{2\gamma}$ as correction to the Coulomb potential, its effect on the nS-state energy level is given by

$$\Delta E_{\text{nS}} = -\frac{|\psi_{\text{nS}}(0)|^2}{4Mm} f_+^{2\gamma}(m), \quad (42)$$

with $|\psi_{\text{nS}}(0)|^2 = \alpha^3 m_r^3 / (\pi n^3)$ - the non-relativistic squared wave function of the hydrogen atom, where $m_r = Mm/(M+m)$ is the reduced mass of the lepton and proton bound state. Using the DR for $f_+^{2\gamma}$ with only the elastic part of the unpolarized cross section and subtracting the accounted TPE contribution in the hydrogen wave functions, as well as the OPE finite size correction, we reproduce the non-relativistic limit of the TPE contribution:

$$\Delta E_{\text{nS}} = -\frac{8m_r^4 \alpha^5}{\pi n^3} \int_0^\infty \frac{dQ^2}{Q^5} (G_E^2(Q^2) - 2G_E'(0)Q^2 - 1). \quad (43)$$

This correction yields the third Zemach moment term [49].

The TPE contribution to the nS-level HFS $\delta E_{\text{nS}}^{\text{HFS}}$ is expressed in terms of the relative correction Δ_{HFS} and the leading order nS-level HFS $E_{\text{nS}}^{\text{HFS},0}$ (Fermi energy) as

$$\delta E_{\text{nS}}^{\text{HFS}} = \Delta_{\text{HFS}} E_{\text{nS}}^{\text{HFS},0}, \quad (44)$$

$$E_{\text{nS}}^{\text{HFS},0} = \frac{8}{3} \frac{m_r^3 \alpha^4 \mu_P}{Mm n^3}. \quad (45)$$

Considering the spin part of $T^{2\gamma}$ as correction to the Hamiltonian of the lepton-proton spin-spin interaction, we express the leading TPE proton structure correction to the S-level HFS in terms of the amplitudes $f_-^{2\gamma}$, $g_-^{2\gamma}$ at threshold ($\omega = m$):

$$\mu_P e^2 \Delta_{\text{HFS}} = -g_-^{2\gamma}(m) + \frac{1}{2} f_-^{2\gamma}(m). \quad (46)$$

The TPE correction to the S-level HFS Δ_0 of Refs. [35–43, 48] can be obtained adding $g_-^{2\gamma}(m) + f_-^{2\gamma}(m) = 0$ to Eq. (46):

$$\mu_P e^2 \Delta_0 = \frac{3}{2} f_-^{2\gamma}(m). \quad (47)$$

Consequently, we have verified the TPE correction to HFS of S energy levels. In the following, we study the difference in the individual channel contribution to HFS correction between the traditional HFS expressions and the DR approach based on the forward lepton-proton amplitudes.

Traditionally the proton intermediate state TPE correction to HFS Δ_0^{el} is expressed as a sum of the Zemach correction Δ_Z with subtraction of the TPE contribution, which is already accounted for in the hydrogen wave functions, and the recoil correction Δ_R^{p} :

$$\Delta_0^{\text{el}} = \Delta_Z + \Delta_R^{\text{p}}, \quad (48)$$

$$\Delta_Z = \frac{8\alpha m_r}{\pi \mu_P} \int_0^\infty \frac{dQ}{Q^2} (G_M(Q^2) G_E(Q^2) - \mu_P), \quad (49)$$

$$\begin{aligned} \Delta_R^{\text{p}} = & \frac{\alpha}{\pi \mu_P} \int_0^\infty \frac{dQ^2}{Q^2} \left\{ \frac{[2 + \rho(\tau_l) \rho(\tau_P)] F_D(Q^2) + 3\rho(\tau_l) \rho(\tau_P) F_P(Q^2)}{\sqrt{\tau_P} \sqrt{1 + \tau_l} + \sqrt{\tau_l} \sqrt{1 + \tau_P}} - \frac{4m_r}{Q} G_E(Q^2) \right\} \\ & \times G_M(Q^2) - \frac{\alpha}{\pi \mu_P} \frac{m}{M} \int_0^\infty \frac{dQ}{Q} \beta_1(\tau_l) F_P^2(Q^2), \end{aligned} \quad (50)$$

with $\beta_1(\tau) = -3\tau + 2\tau^2 + 2(2 - \tau)\sqrt{\tau(1 + \tau)}$ [42].

We express the elastic TPE contribution to the S-level HFS $\Delta_{\text{HFS}}^{\text{el}}$ in the lepton-proton amplitudes DR framework with subtraction of the TPE contribution, which is already accounted for in the hydrogen wave functions, in terms of the proton electric and magnetic form factors as

$$\Delta_{\text{HFS}}^{\text{el}} = \frac{\alpha}{\pi \mu_P} \int_0^\infty \frac{dQ^2}{Q^2} \left\{ \frac{2G_E(Q^2) + \rho(\tau_l) \rho(\tau_P) G_M(Q^2)}{\sqrt{\tau_P} \sqrt{1 + \tau_l} + \sqrt{\tau_l} \sqrt{1 + \tau_P}} G_M(Q^2) - \frac{4\mu_P m_r}{Q} \right\}. \quad (51)$$

We reproduce the Zemach correction [34] as the non-relativistic limit of the elastic TPE correction $\Delta_{\text{HFS}}^{\text{el}}$. The non-pole term:

$$\Delta_{\text{HFS}}^{\text{F}_P^2} = \frac{\alpha}{\pi \mu_P} \frac{m}{M} \int_0^\infty \frac{dQ}{Q} \beta_1(\tau_l) F_P^2(Q^2), \quad (52)$$

was eliminated from the TPE contribution to HFS in Refs. [42, 43], see last term in Eq. (48). In our approach the non-pole term does not appear and, therefore, does not need to

be subtracted by hand. The remaining difference between expressions of Eq. (48) and Eq. (51) is given by the elastic contribution to the amplitude $g^{2\gamma}(m) + f_-^{2\gamma}(m)$.

Traditionally the polarizability correction Δ_0^{pol} is given by [42, 43]

$$\begin{aligned} \Delta_0^{\text{pol}} = & \frac{2\alpha}{\pi\mu_P} \int_0^\infty \frac{dQ^2}{Q^2} \int_{\nu_{\text{thr}}^{\text{inel}}}^\infty \frac{d\nu_\gamma}{\nu_\gamma} \frac{[2 + \rho(\tau_l) \rho(\tilde{\tau})] g_1(\nu_\gamma, Q^2) - 3\rho(\tau_l) \rho(\tilde{\tau}) g_2(\nu_\gamma, Q^2) / \tilde{\tau}}{\sqrt{\tilde{\tau}}\sqrt{1+\tau_l} + \sqrt{\tau_l}\sqrt{1+\tilde{\tau}}} \\ & + \frac{\alpha}{\pi\mu_P} \frac{m}{M} \int_0^\infty \frac{dQ}{Q} \beta_1(\tau_l) F_P^2(Q^2). \end{aligned} \quad (53)$$

We express the inelastic α^5 -correction to the S-level HFS in the lepton-proton amplitudes DR approach in terms of the proton inelastic spin SFs g_1 and g_2 as

$$\Delta_{\text{HFS}}^{\text{inel}} = \frac{2\alpha}{\pi\mu_P} \int_0^\infty \frac{dQ^2}{Q^2} \int_{\nu_{\text{thr}}^{\text{inel}}}^\infty \frac{d\nu_\gamma}{\nu_\gamma} \frac{[2 + \rho(\tau_l) \rho(\tilde{\tau})] g_1(\nu_\gamma, Q^2) + [2 - \rho(\tau_l) \rho(\tilde{\tau}) / \tilde{\tau}] g_2(\nu_\gamma, Q^2)}{\sqrt{\tilde{\tau}}\sqrt{1+\tau_l} + \sqrt{\tau_l}\sqrt{1+\tilde{\tau}}}. \quad (54)$$

It differs from Δ_0^{pol} by the absence of the $\Delta_{\text{HFS}}^{\text{F}_P^2}$ contribution, which allows to expand the HFS integrand near $Q^2 = 0$ in terms of polarizabilities, and by the contribution from the spin SF g_2 to the amplitude $g^{2\gamma}(m) + f_-^{2\gamma}(m)$.

Consequently, the resulting TPE correction to HFS of S energy levels can be equivalently expressed as

$$\Delta_{\text{HFS}} = \Delta_{\text{HFS}}^{\text{el}} + \Delta_{\text{HFS}}^{\text{inel}} = \Delta_Z + \Delta_R^{\text{p}} + \Delta_0^{\text{pol}} = \Delta_0. \quad (55)$$

A. Resulting HFS correction evaluation

For the numerical evaluation of the TPE corrections to HFS from the proton intermediate state and the $\Delta_{\text{HFS}}^{\text{F}_P^2}$ part of the polarizability correction Δ_0^{pol} we exploit the elastic form factor parametrizations from Refs. [12, 13]. For the Zemach correction we make two evaluations for the 1- σ band curves coming from the elastic proton form factor uncertainties of Refs. [12, 13], where a global analysis of the electron-proton scattering data with account of TPE corrections for $Q^2 < 10 \text{ GeV}^2$ was performed, and estimate the uncertainty as a half of a difference between these two curves. For the numerical evaluation of the inelastic correction we exploit the spin SFs data parametrization from Refs. [62–64] in the region of large Q^2 . In the region of low Q^2 , we expand the Q^2 -integrand from the proton spin SFs in terms of small x_{Bj} and account for the leading non-vanishing moments:

$$\begin{aligned} \Delta_0^{\text{pol}} \rightarrow & \frac{\alpha}{2\pi} \int_0^\infty dQ^2 \frac{\rho(\tau_l) (\rho(\tau_l) - 4)}{\mu_P M m \tau_l} I_1(Q^2) + \frac{\alpha}{8\pi} \int_0^\infty dQ^2 \frac{(9 - 2\rho(\tau_l)) \rho(\tau_l)^2}{\mu_P M m \tau_l} I_1^{(3)}(Q^2) \\ & - \frac{3\alpha}{2\pi} \int_0^\infty dQ^2 \frac{1 + 2\rho(\tau_l)}{\mu_P M m} I_2^{(3)}(Q^2), \end{aligned} \quad (56)$$

$$\Delta_{\text{HFS}}^{\text{inel}} \rightarrow \Delta_0^{\text{pol}} - \frac{2\alpha}{\pi} \int_0^\infty dQ^2 \frac{\rho(\tau_l)}{\mu_P M m \tau_l} I_2(Q^2), \quad (57)$$

with the moments of the proton spin SFs:

$$I_1(Q^2) = \frac{2M^2}{Q^2} \int_0^{x_{\text{thr}}^{\text{inel}}} g_1(x_{\text{Bj}}, Q^2) dx_{\text{Bj}}, \quad I_1(0) = -\frac{(\mu_P - 1)^2}{4}, \quad (58)$$

$$I_2(Q^2) = \frac{2M^2}{Q^2} \int_0^{x_{\text{thr}}^{\text{inel}}} g_2(x_{\text{Bj}}, Q^2) dx_{\text{Bj}} = \frac{1}{4} F_P(Q^2) G_M(Q^2), \quad (59)$$

$$I_1^{(3)}(Q^2) = \frac{8M^4}{Q^4} \int_0^{x_{\text{thr}}^{\text{inel}}} x_{\text{Bj}}^2 g_1(x_{\text{Bj}}, Q^2) dx_{\text{Bj}} \xrightarrow{Q^2 \rightarrow 0} \frac{Q^2 M^2}{2\alpha} \gamma_0, \quad (60)$$

$$I_2^{(3)}(Q^2) = \frac{8M^4}{Q^4} \int_0^{x_{\text{thr}}^{\text{inel}}} x_{\text{Bj}}^2 g_2(x_{\text{Bj}}, Q^2) dx_{\text{Bj}} \xrightarrow{Q^2 \rightarrow 0} \frac{Q^2 M^2}{2\alpha} (\delta_{\text{LT}} - \gamma_0), \quad (61)$$

with $x_{\text{thr}}^{\text{inel}} = Q^2/(2M\nu_{\text{thr}}^{\text{inel}})$ and the low-energy constants values [65–70]:

$$\delta_{\text{LT}} = (1.34 \pm 0.17) \times 10^{-4} \text{ fm}^4, \quad (62)$$

$$\gamma_0 = (-1.01 \pm 0.13) \times 10^{-4} \text{ fm}^4, \quad (63)$$

$$I'_1(0) = (7.6 \pm 2.5) \text{ GeV}^{-2}. \quad (64)$$

In Fig. 3 we show the integrand $I_{\text{HFS}}(Q)$ entering the TPE correction:

$$\Delta_{\text{HFS}} = \int_0^\infty I_{\text{HFS}}(Q) dQ, \quad (65)$$

in the case of $e\text{H}$ and μH . The low- Q behavior based on the moments of the proton spin SFs of Eqs. (58, 59–61) $I_{\text{HFS}}^{\text{sr}}$ and the high- Q behavior based on the data $I_{\text{HFS}}^{\text{d}}$ are almost independent of the way to evaluate the TPE correction. While in the region $0.2 \text{ GeV} \lesssim Q \lesssim 0.5 \text{ GeV}$ the HFS evaluation with the DRs for the lepton-proton amplitudes ($\Delta_{\text{HFS}} = \Delta_{\text{HFS}}^{\text{el}} + \Delta_{\text{HFS}}^{\text{inel}}$) and the traditional HFS evaluation ($\Delta_{\text{HFS}} = \Delta_0 = \Delta_0^{\text{el}} + \Delta_0^{\text{pol}}$) slightly differ (for $Q > 0.5 \text{ GeV}$ both methods agree within 2.5%). New data in this kinematical region will be very useful for such evaluation. In order to avoid any model dependence, we connect the two model-independent regions by the function of the Fermi-Dirac distribution type:

$$I_{\text{HFS}}(Q) = I_{\text{HFS}}^{\text{sr}}(Q) \Theta(Q_{\text{sr}} - Q) + I_{\text{HFS}}^{\text{d}}(Q) \Theta(Q - Q_{\text{d}}) + \frac{c_1 I_{\text{HFS}}^{\text{sr}}(Q) + c_2 f(Q) I_{\text{HFS}}^{\text{d}}(Q)}{1 + f(Q)} \Theta(Q - Q_{\text{sr}}) \Theta(Q_{\text{d}} - Q), \quad (66)$$

with $f(Q)$ given by

$$f(Q) = e^{\frac{2Q - Q_{\text{sr}} - Q_{\text{d}}}{2a_0}}. \quad (67)$$

Furthermore, $Q_{\text{sr}} = 0.2 \text{ GeV}$, $Q_{\text{d}} = 0.5 \text{ GeV}$, $a_0 = 0.1 \text{ GeV}$, and the constants c_1 , c_2 , Q_{sr} , a_0 were chosen as those that preserve the regularity and smoothness of the integrand $I_{\text{HFS}}(Q)$.

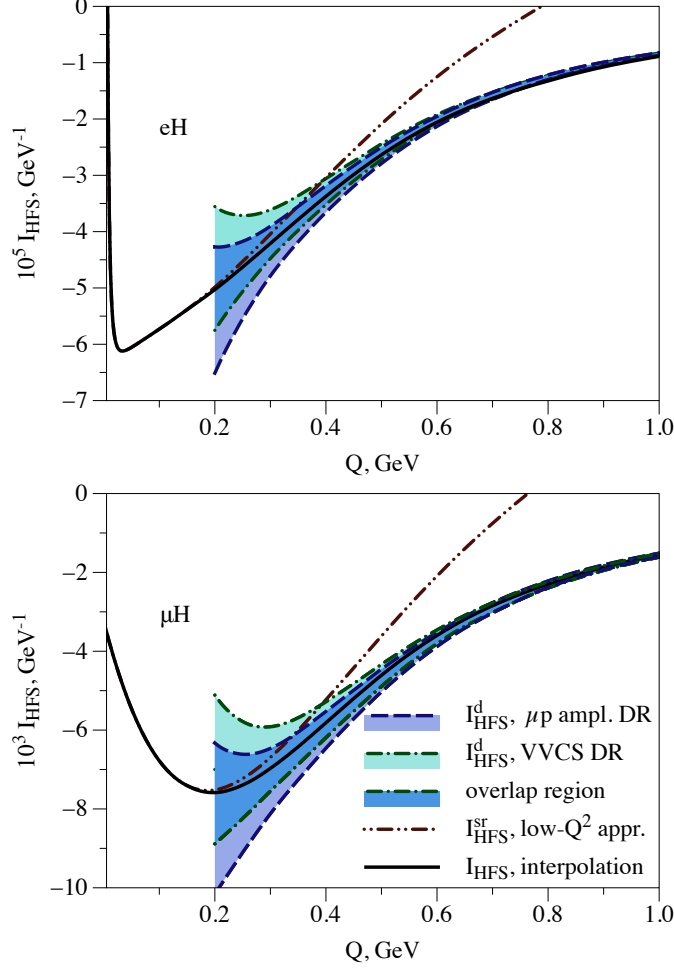


FIG. 3: Q -dependence of the integrand $I_{\text{HFS}}(Q)$ entering the TPE correction to HFS. A comparison is given for the integrands based on the DRs for the lp amplitudes and based on the forward double virtual Compton scattering (VVCS) amplitudes. Upper panel: electronic hydrogen, lower panel: muonic hydrogen.

In the low- Q region, we make two evaluations for the $1\text{-}\sigma$ bands of the elastic proton form factors from Refs. [12, 13]. We add the combined uncertainty from γ_0 , δ_{LT} , $I'_1(0)$ linearly to the form factors uncertainty. For the larger $Q > (0.013 - 0.017)$ GeV, we make evaluation for the central values of the proton elastic form factors and add the uncertainty of the proton elastic form factors to the uncertainties from γ_0 , δ_{LT} , $I'_1(0)$ in quadrature. The boundary Q value is chosen as the value that leads to the same uncertainties in the proton intermediate state HFS contribution in both ways of the error estimate described in this paragraph. For the larger $Q > 0.5$ GeV region, we add the uncertainty of the proton spin structure function parametrization in quadrature to the uncertainties coming from the proton elastic form factors. We connect the high- Q integrands I^d by two curves to the $1\text{-}\sigma$ boundaries in the low- Q region I^{sr} . We estimate the uncertainty from the difference between the integral of Eq. (65) for these two curves, which are shown in Fig. 4 for eH (μH), and take the averaged central value. In the region $Q^2 > 10$ GeV², the sizable contribution comes only from the μ_P term in Eqs. (49-51) and doesn't introduce any sizable additional uncertainty.

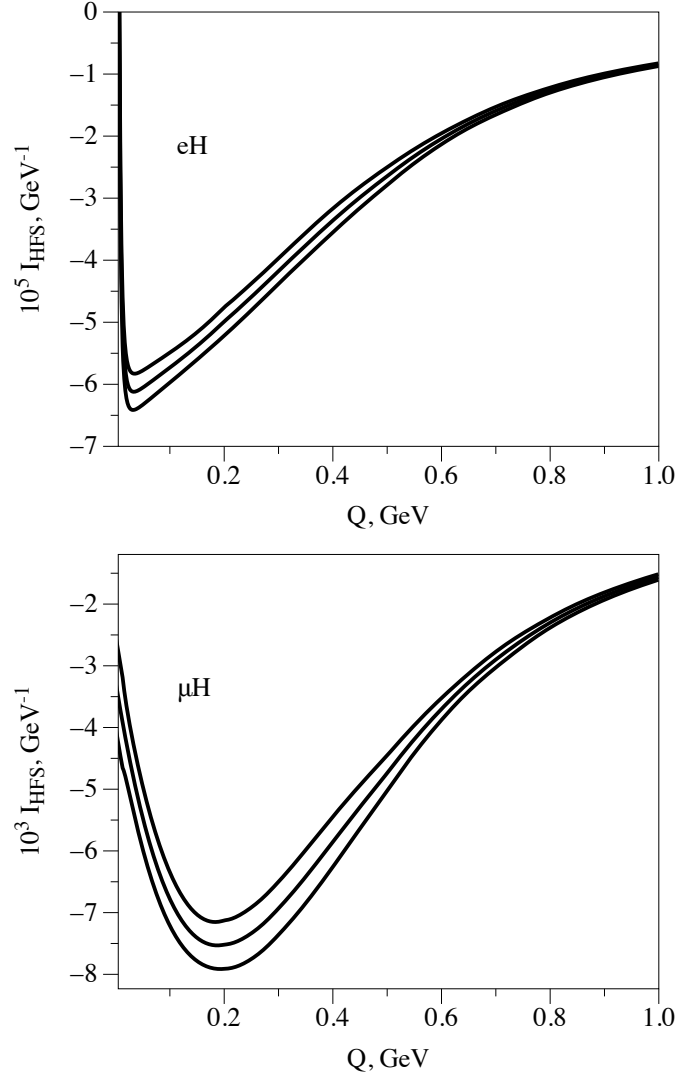


FIG. 4: HFS integrand $I_{\text{HFS}}(Q)$ in the evaluation by the DRs for lp amplitudes with error bands. Upper panel: electronic hydrogen, lower panel: muonic hydrogen.

We evaluate the proton TPE correction to HFS in the DR approach either for the forward double virtual Compton scattering (TPE correction of Refs. [42, 43]) or for the lepton-proton amplitudes and present results for the Zemach correction, the recoil correction and the $\Delta_{\text{HFS}}^{\text{F}_2^{\text{p}}}$ contribution in Table I. We also present the result of the polarizability correction Δ_0^{pol} , which evaluation will be described in Section IV C. The evaluation of the resulting TPE correction is performed for the sum of elastic and inelastic contributions using the traditional expressions and the expressions based on the DRs for lp amplitudes. The latter leads to twice smaller uncertainties. However, both evaluations agree within errors, which is a good test of the proton spin structure function g_2 parametrization for this calculation, and agree with the traditional evaluation of a sum $\Delta_0^{\text{el}} + \Delta_0^{\text{pol}}$. The leading Zemach correction is a bit smaller than the result based on the typical proton form factors parametrization in Ref. [42] due to the suppressed low- Q^2 behavior of the magnetic proton form factor measured by the A1 Collaboration at MAMI [12, 13].

	$10^6 \Delta, eH$	$10^3 \Delta, \mu H$
Zemach, Δ_Z	$-39.59(75)$	$-7.36(14)$
Recoil, Δ_R^p	$5.31(7)$	$0.8476(84)$
Traditional elastic, Δ_0^{el}	$-34.29(75)$	$-6.51(14)$
Total elastic, $\Delta_{\text{HFS}}^{\text{el}}$	$-43.40(74)$	$-7.03(14)$
Non-pole term, $\Delta_{\text{HFS}}^{\text{F}_P^2}$	$22.53(7)$	$1.11(1)$
Polarizability, Δ_0^{pol}	$1.91(51)$	$0.363(86)$
Total Δ_{HFS} , within VVCS DRs	$-32.60(2.56)$	$-6.18(49)$
Total Δ_{HFS} within lp DRs	$-32.80(1.56)$	$-6.22(29)$
Total, $\Delta_{\text{HFS}} = \Delta_0^{\text{el}} + \Delta_0^{\text{pol}}$ [42]	$-32.38(91)$	$-6.15(16)$

TABLE I: Finite-size TPE correction to the hyperfine splitting of S energy levels in eH and μH . The Fermi energy HFS is $5.86785 \mu\text{eV}$ for the 1S level in eH and 182.4432 meV for the 1S level in μH .

The evaluation of the elastic Δ_0^{el} and polarizability Δ_0^{pol} corrections in sum [42] has smaller uncertainty than the evaluation of the total TPE correction described above. However, we do not account for the third moments of the proton spin structure functions in the described above method and also add uncertainties coming from two integration regions in quadrature, while in the first method the integration of the resulting uncertainty is performed.

B. Zemach correction evaluation

The Zemach correction can be evaluated accounting for the measured values of the proton charge and magnetic radii. We split the Q -integration in the Zemach contribution at a small enough scale Q_0 and exploit the radii expansion at low Q^2 as

$$\Delta_Z = \frac{8\alpha m_r}{\pi} \left(\int_{Q_0}^{\infty} \frac{dQ}{Q^2} \left(\frac{G_M(Q^2) G_E(Q^2)}{\mu_P} - 1 \right) - \frac{r_E^2 + r_M^2}{6} Q_0 \right), \quad (68)$$

with the approximate value $Q_0 \lesssim (0.1 - 0.2) \text{ GeV}$ and the definition of the proton radii:

$$r_{E(M)}^2 = -\frac{6}{G_{E(M)}(0)} \left. \frac{dG_{E(M)}(Q^2)}{dQ^2} \right|_{Q^2=0}. \quad (69)$$

The resulting uncertainty is evaluated as a sum of the form factors uncertainty [13] and radii uncertainties in quadrature. Substituting values for the magnetic proton radius $r_M = 0.799 \pm 0.017 \text{ fm}$ and the electric radius $r_E = 0.879 \pm 0.008 \text{ fm}$ from the electron-proton scattering data [13] and requiring the minimal uncertainty of the Zemach correction by choice $Q_0^2 = 0.018 \text{ GeV}^2$, we obtain for the Zemach correction $\Delta_Z = -7422 \pm 58 \text{ ppm}$ and for the resulting TPE correction $\Delta_{\text{HFS}} = -6212 \pm 104 \text{ ppm}$. With the substitution of the electric charge radius $r_E = 0.84087 \pm 0.00039 \text{ fm}$ from the muonic hydrogen spectroscopy experiments [11] and $Q_0^2 = 0.0285 \text{ GeV}^2$ the Zemach correction is given by $\Delta_Z = -7374 \pm 46 \text{ ppm}$ leading to the resulting HFS correction $\Delta_{\text{HFS}} = -6164 \pm 98 \text{ ppm}$.

C. Polarizability correction evaluation

For the numerical evaluation of the polarizability correction we subtract the leading moment of the spin structure function g_1 and separate contributions from the g_1 and g_2 structure functions as [49]

$$\Delta_0^{\text{pol}} = \Delta_1^{\text{pol}} + \Delta_2^{\text{pol}}, \quad (70)$$

$$\Delta_1^{\text{pol}} = \frac{\alpha}{\pi\mu_P} \frac{m}{M} \int_0^\infty \frac{dQ}{Q} \beta_1(\tau_l) \{4I_1(Q^2) + F_P^2(Q^2)\} \\ + \frac{2\alpha}{\pi\mu_P} \int_0^\infty \frac{dQ^2}{Q^2} \int_{\nu_{\text{thr}}^{\text{inel}}}^\infty \frac{d\nu_\gamma}{\nu_\gamma} \left\{ \frac{2 + \rho(\tau_l)\rho(\tilde{\tau})}{\sqrt{\tilde{\tau}}\sqrt{1+\tau_l} + \sqrt{\tau_l}\sqrt{1+\tilde{\tau}}} - \frac{m\beta_1(\tau_l)}{\nu_\gamma} \right\} g_1(\nu_\gamma, Q^2), \quad (71)$$

$$\Delta_2^{\text{pol}} = -\frac{6\alpha}{\pi\mu_P} \int_0^\infty \frac{dQ^2}{Q^2} \int_{\nu_{\text{thr}}^{\text{inel}}}^\infty \frac{d\nu_\gamma}{\nu_\gamma \tilde{\tau}} \frac{\rho(\tau_l)\rho(\tilde{\tau})g_2(\nu_\gamma, Q^2)}{\sqrt{\tilde{\tau}}\sqrt{1+\tau_l} + \sqrt{\tau_l}\sqrt{1+\tilde{\tau}}}, \quad (72)$$

with the first moment of the g_1 structure function given by Eq. (58).

In order to evaluate the contribution from $4I_1 + F_P^2$ we approximate $I_1(Q^2) = I_1(0) + I_1'(0)Q^2$ up to $Q_{I_1} = 0.25$ GeV, with the low-energy constant $I_1'(0) = (7.6 \pm 2.5)$ GeV⁻² [65], and afterward we exploit the spin SFs data parametrization from Refs. [62–64] (JLab parametrization). We show the correspondent Q^2 dependence of $4I_1 + F_P^2$ contribution in Fig. 5.

For the remaining polarizability corrections Δ_1^{pol} and Δ_2^{pol} coming from g_1 and g_2 we use the JLab parametrization only, which is in a fair agreement with the MAID model [66, 67] in the region of low Q^2 , see Fig. 6 for details.

We add the uncertainties coming from the Pauli form factor F_P [12, 13], spin structure functions g_1 , g_2 and the parameter $I_1'(0)$ in quadrature under the HFS integrand and treat the uncertainties coming from the two Q integration regions in the Δ_1 and $4I_1 + F_P^2$ contributions as uncorrelated uncertainties.

We present the results for the TPE contribution to the 1S energy level HFS in eH (2S in μ H) in Table II (III). Though the contributions from the g_1 and g_2 structure functions slightly differ with a previous evaluation of Ref. [43], the resulting polarizability correction is in agreement with results of Ref. [43]: $\Delta_0^{\text{pol}} = 11.0 \pm 3.8$ peV in eH and $\Delta_0^{\text{pol}} = 8.0 \pm 2.6$ μ eV in μ H.

eH	$4I_1 + F_P^2$	g_1	Δ_1^{pol}	Δ_2^{pol}	Δ_0^{pol}
ΔE_{1S} , peV	11.6 ± 2.8	1.17 ± 0.65	13.8 ± 2.8	-2.61 ± 0.8	11.2 ± 3.0

TABLE II: Contributions to the 1S HFS TPE correction in eH.

μ H	$4I_1 + F_P^2$	g_1	Δ_1^{pol}	Δ_2^{pol}	Δ_0^{pol}
ΔE_{2S} , μ eV	9.17 ± 2.09	0.61 ± 0.35	9.78 ± 1.91	-1.48 ± 0.44	8.30 ± 1.96

TABLE III: Contributions to the 2S HFS TPE correction in μ H.

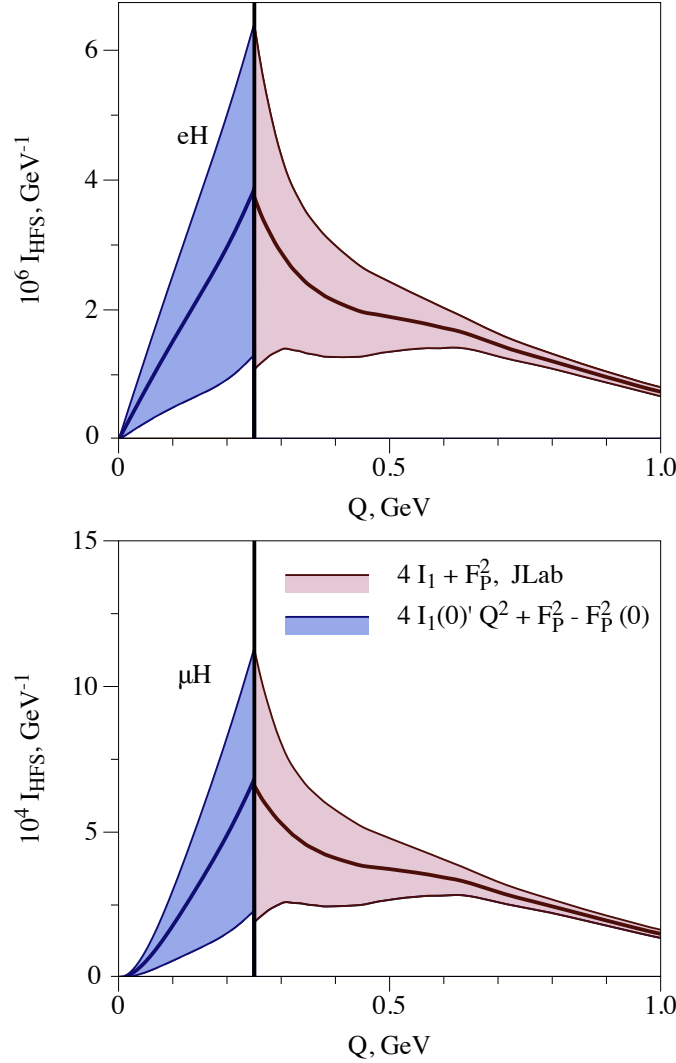


FIG. 5: JLab HFS integrand from $4I_1 + F_P^2$, corresponding with the first integral in Eq. (71), connected to the low- Q^2 behavior. Upper panel: electronic hydrogen, lower panel: muonic hydrogen.

Now we study the polarizability correction to HFS in μH in detail. The result in Table III corresponds to the relative correction $\Delta_0^{\text{pol}} = 363 \pm 86$ ppm. The account of the third moments of the spin structure functions in the low- Q^2 integration region increases the polarizability correction resulting in $\Delta_0^{\text{pol}} = 395 \pm 103$ ppm. The larger central value of the correction is explained by the anomalous change of sign in the low- Q^2 behavior of the g_2 contribution, see Fig. 7, as well as by the increased contribution from the g_1 structure function. In the following Fig. 8 we compare the contribution of the $4I_1 + F_P^2$ as well as the contribution of the next term in the moments expansion with the total polarizability integrand. The main uncertainty comes from the pure knowledge of $I_1(0)'$. The contribution from the low-energy constants γ_0 and δ_{LT} is below the uncertainty level, as it is shown in Fig. 8.

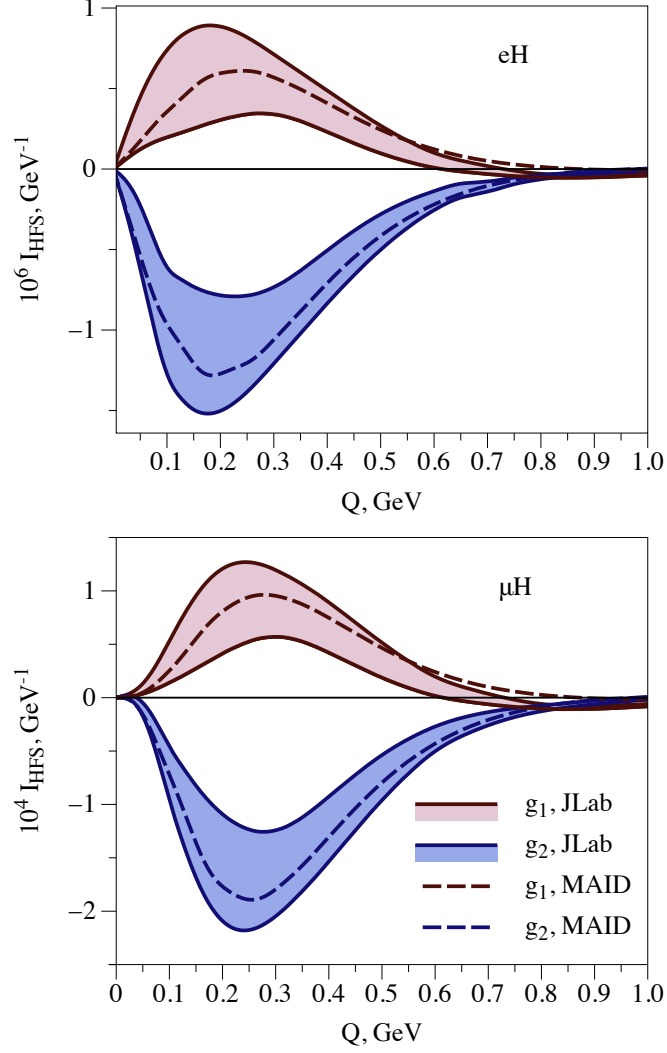


FIG. 6: MAID and JLab integrand in the g_1 integral of Eq. (71) and the g_2 integral of Eq. (72). Upper panel: electronic hydrogen, lower panel: muonic hydrogen.

Within the dispersion relation approach, see Eqs. (16, 47), we express the polarizability correction Δ_0^{pol} directly in terms of the measurable inclusive inelastic lp cross sections as

$$\Delta_0^{\text{pol}} = \frac{3Mm}{\pi e^2 \mu_P} \int_{\omega_{\text{thr}}}^{\infty} \frac{\sigma_{++}^{\text{inel}}(\omega') - \sigma_{+-}^{\text{inel}}(\omega')}{\sqrt{\omega'^2 - m^2}} d\omega' + \frac{\alpha}{\pi \mu_P} \frac{m}{M} \int_0^{\infty} \frac{dQ}{Q} \beta_1(\pi) F_P^2(Q^2), \quad (73)$$

with the pion production threshold $\omega_{\text{thr}} = m + m_\pi(2M + 2m + m_\pi)/(2M)$.

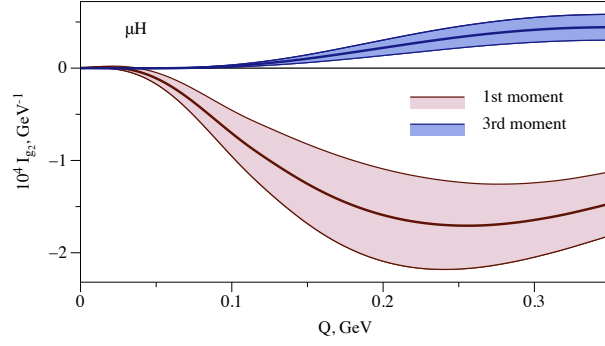


FIG. 7: Contribution of the g_2 structure function to the HFS integrand $I_{\text{HFS}}(Q)$ in muonic hydrogen when the first moment or the third moment are replaced by the low-energy constants, 0 and $\delta_{\text{LT}} - \gamma_0$ respectively.

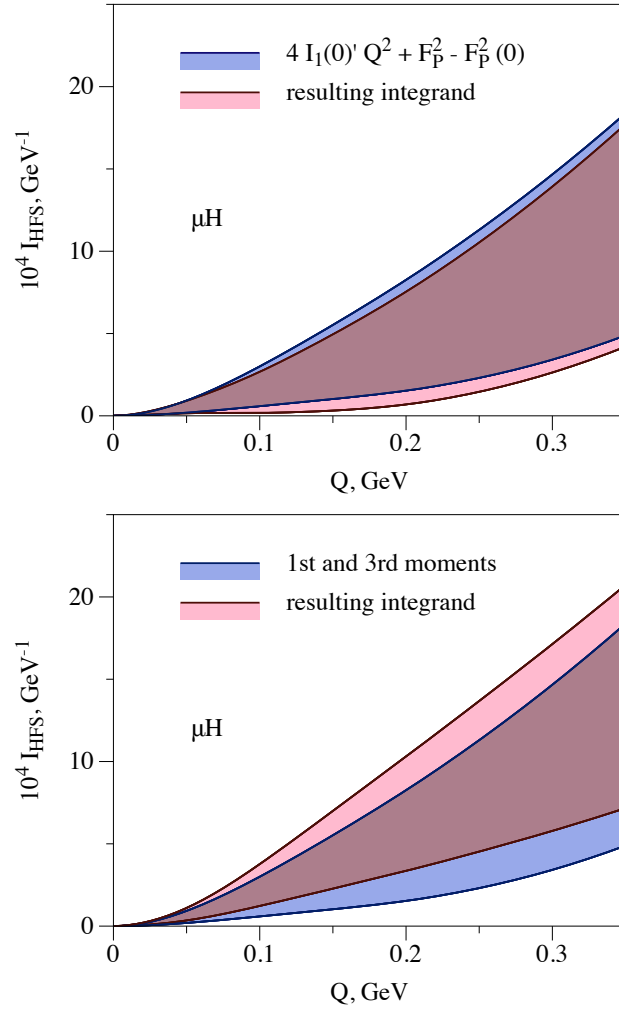


FIG. 8: Upper panel: Relative contribution of $4I_1 + F_P^2$ to the HFS integrand in muonic hydrogen. Lower panel: Relative contribution of $4I_1 + F_P^2$ and third moments of the proton spin structure functions to the HFS integrand in muonic hydrogen.

V. CONCLUSIONS AND OUTLOOK

In this work we have derived DRs for the forward lepton-proton scattering TPE amplitudes. We have fully expressed the spin-dependent TPE amplitudes in terms of the inclusive total cross sections at the leading α order or equivalently in terms of the proton spin SFs. With these relations we have found a new way to determine the $O(\alpha^5)$ TPE proton structure correction to the S-level HFS in the hydrogen-like atoms explicitly accounting for the helicity double spin-flip amplitude. The result for individual channel HFS contribution is distinct to the standard approach, e.g., the elastic TPE contribution to HFS differs by the finite sizable correction. Only accounting for contributions from all possible channels through the Burkard-Cottingham sum rule both methods agree. The polarizability correction was expressed in terms of the experimentally measurable inclusive cross-sections. We have reevaluated the TPE correction to HFS in electronic and muonic hydrogen connecting the region with small photons virtualities, which is expressed through the first and third moments of the proton spin SFs, to the region with large photons virtualities, where the data (parametrizations) on the proton form factors and SFs exists. The resulting TPE correction is similar to the literature result with slightly larger uncertainties in the standard approach to HFS and slightly smaller uncertainties within our approach. The smallest uncertainty is obtained by the evaluation of the proton Δ_0^{el} and polarizability Δ_0^{pol} corrections separately expressing the region of small virtualities through the proton low-energy constants.

In view of the forthcoming high-precision measurements of the 1S HFS in muonic hydrogen with 1 ppm precision level [16, 18, 19], we also provide the corresponding best estimates of the HFS correction from the TPE graph in Table IV. The uncertainty of our estimate is 100 times larger than the expected experimental accuracy. The uncertainty of the polarizability contribution is almost 2 times larger than the uncertainty of the Zemach term and dominated by pure knowledge of $I'_1(0)$. The forthcoming data from EG4, SANE and g2p experiments at JLab on the proton spin structure functions g_1 , g_2 [45–47] will improve the knowledge of the polarizability correction. The precise measurements of the proton magnetic form factors at low Q^2 [44] will allow to decrease the uncertainty of the Zemach term.

	Δ (ppm), μH	uncertainty (ppm)
Zemach, Δ_Z	−7374	46
Recoil, Δ_R^{p}	847.6	8.4
Polarizability, Δ_0^{pol}	363	86
Total, $\Delta_{\text{HFS}} = \Delta_0^{\text{el}} + \Delta_0^{\text{pol}}$	−6164	98

TABLE IV: Finite-size TPE correction to the hyperfine splitting of the S energy levels in μH .

Consequently after accounting for all contributions at the 1 – 10 ppm level, the forthcoming measurements can constrain the low- Q^2 TPE contribution to HFS $\Delta_{\text{structure}}$ with the following combination of the proton radii and $I'_1(0)$:

$$\Delta_{\text{structure}} = -\frac{4\alpha}{3\pi} \left(m_r Q_0 (r_E^2 + r_M^2) + \frac{m}{M} \frac{h(\tau_l)}{\mu_P} I'_1(0) m^2 \right), \quad (74)$$

with

$$h(\tau) = (9 - 4\tau) \tau^2 + \frac{15}{2} \ln \left(\sqrt{\tau} + \sqrt{1 + \tau} \right) - \frac{1}{2} (15 + 22\tau - 8\tau^2) \sqrt{\tau(1 + \tau)}, \quad (75)$$

and τ_l is taken at the point $Q = Q_{I_1} \sim (0.1 - 0.3) \text{ GeV}$ up to which we use the low-energy expansion of $I_1(Q^2)$.

VI. ACKNOWLEDGMENTS

We thank Vladimir Pascalutsa for useful discussions about general formalism and advices given during this work and manuscript preparation, Marc Vanderhaeghen for useful discussions and advices concerning the numerical evaluations, Carl Carlson for the discussions concerning literature. We thank Keith Griffioen, Sebastian Kuhn, Nevzat Guler and Jacob Ethier for providing us with results on the proton spin SFs and Slava Tsaran for his script for an online access of MAID. This work was supported by the Deutsche Forschungsgemeinschaft (DFG) through Collaborative Research Center “The Low-Energy Frontier of the Standard Model” (SFB 1044), and Graduate School “Symmetry Breaking in Fundamental Interactions” (DFG/GRK 1581).

Appendix A: Crossing in lepton-proton scattering

In order to establish the even-odd properties for the invariant amplitudes under the crossing $\omega \rightarrow -\omega$, we first perform the crossing on the lepton line and relate the amplitudes of the lepton-proton scattering $f^{l^-p}(\omega)$ in the physical region ($\omega > 0$) to the amplitudes of the antilepton-proton scattering $f^{l^+p}(-\omega)$ in the unphysical region ($\omega < 0$). Writing the general form of the amplitude as

$$T_{h'\lambda',h\lambda}(\omega) = \sum_{i=1}^3 A_i(\omega) \bar{u}(k, h') O_i u(k, h) \bar{N}(p, \lambda') O_i N(p, \lambda), \quad (\text{A1})$$

with $O = (1, \gamma^{\mu\nu}, \gamma^\mu \gamma_5)$. We observe that after the replacement in the lepton line $k \rightarrow -k$, the amplitude transforms to

$$T_{h'\lambda',h\lambda}^c(\omega) = \sum_{i=1}^3 A_i(-\omega) \bar{u}(-k, -h') O_i u(-k, -h) \bar{N}(p, \lambda') O_i N(p, \lambda). \quad (\text{A2})$$

We can rewrite the lepton spinor u in terms of the antilepton spinor v as $u(-k, -h) = \gamma^2 v^*(k, h)$, where we exploit the same form u for the antilepton spinor as only particles or antiparticles participate in interaction. The expression for the helicity amplitude is given by

$$T_{h'\lambda',h\lambda}^c(\omega) = \sum_{i=1}^3 A_i(-\omega) v^T(k, h') \gamma_2^+ \gamma_0 O_i \gamma_2 v^*(k, h) \bar{N}(p, \lambda') O_i N(p, \lambda). \quad (\text{A3})$$

Transposing the lepton line we obtain:

$$T_{h'\lambda',h\lambda}^c(\omega) = \sum_{i=1}^3 A_i(-\omega) \bar{v}(k, h) \gamma_0 (\gamma_2^+ \gamma_0 O_i \gamma_2)^T v(k, h') \bar{N}(p, \lambda') O_i N(p, \lambda). \quad (\text{A4})$$

The tensor structure of Eq. (3) transforms to

$$\begin{aligned}
T_{h'\lambda',h\lambda}^c(\omega) = & -\frac{f_+(-\omega)}{4Mm} \bar{v}(k,h)v(k,h') \bar{N}(p,\lambda')N(p,\lambda) \\
& - \frac{mf_-(-\omega) - \omega g(-\omega)}{8M\vec{k}^2} \bar{v}(k,h)\gamma^{\mu\nu}v(k,h') \bar{N}(p,\lambda')\gamma_{\mu\nu}N(p,\lambda) \\
& - \frac{-\omega f_-(-\omega) + mg(-\omega)}{4M\vec{k}^2} \bar{v}(k,h)\gamma_\mu\gamma_5v(k,h') \bar{N}(p,\lambda')\gamma^\mu\gamma_5N(p,\lambda), \quad (\text{A5})
\end{aligned}$$

which corresponds to the scattering of the antilepton off the proton.

According to the crossing properties we can write amplitudes for the scattering of the antilepton f^{l+p} in terms of the lepton scattering amplitudes f^{l-p} as

$$f_+^{l+p}(\omega) = f_+^{l-p}(-\omega), \quad (\text{A6})$$

$$f_-^{l+p}(\omega) = -f_-^{l-p}(-\omega), \quad (\text{A7})$$

$$g^{l+p}(\omega) = g^{l-p}(-\omega). \quad (\text{A8})$$

Appendix B: Dispersion relations verification in QED

In this Appendix, we verify the lepton-proton forward dispersion relations in QED. We reconstruct the real parts of the TPE amplitudes with the relations of Eqs. (16-18) and compare them with the sum of the direct and crossed box graphs. The OPE helicity amplitude $T_{h'\lambda'h\lambda}^{1\gamma}$ for the lepton scattering off the charged point proton: $l(k,h) + p(p,\lambda) \rightarrow l(k',h') + p(p',\lambda')$, where $h(h')$ denote the incoming (outgoing) lepton helicities and $\lambda(\lambda')$ the corresponding proton helicities respectively, see Fig. 9, is given by

$$T_{h'\lambda'h\lambda}^{1\gamma} = \frac{e^2}{Q^2 + \mu^2} \bar{u}(k',h')\gamma^\mu u(k,h) \bar{N}(p',\lambda')\gamma_\mu N(p,\lambda). \quad (\text{B1})$$

We introduce the finite photon mass μ with the aim to have no deal with IR divergences. Such process is completely described by 2 Mandelstam variables, e.g., $Q^2 = -(k - k')^2$ - the squared momentum transfer, and $s = (p + k)^2 = M^2 + 2M\omega + m^2$ - the squared energy in the lepton-proton c.m. reference frame.

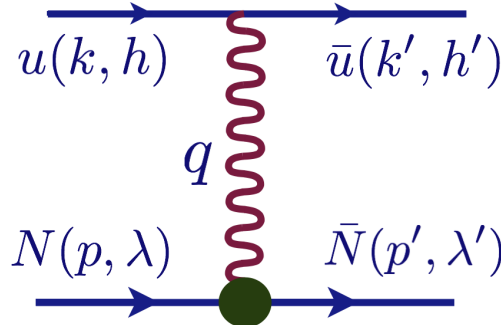


FIG. 9: One photon exchange graph.

The relevant OPE cross sections are given by

$$\sigma^{1\gamma}(\omega) = \frac{4\pi M^2 \alpha^2}{\Sigma_s} \left\{ \frac{\Sigma_s}{2M^2 s} + \left(\frac{s}{M^2} + \frac{4\omega^2}{\mu^2} + \frac{\mu^2}{2M^2} \right) \frac{\Sigma_s}{\Sigma_s + s\mu^2} - \frac{s + \mu^2}{M^2} \ln \frac{\Sigma_s + s\mu^2}{s\mu^2} \right\}, \quad (\text{B2})$$

$$\sigma_{++}^{1\gamma}(\omega) - \sigma_{+-}^{1\gamma}(\omega) = \frac{16\pi M \alpha^2}{\Sigma_s^2} \left\{ (\omega \Sigma_s + 2\mu^2(m^2 + M\omega)(\omega + M)) \ln \frac{\Sigma_s + s\mu^2}{s\mu^2} - \frac{\Sigma_s (\Sigma_s (2\omega s - M(\omega^2 - m^2)) + 2s(m^2 + M\omega)(\omega + M)\mu^2)}{s(\Sigma_s + s\mu^2)} \right\}, \quad (\text{B3})$$

$$\sigma_{\perp}^{1\gamma}(\omega) - \sigma_{\parallel}^{1\gamma}(\omega) = \frac{4\pi \alpha^2 M m}{\Sigma_s^2} \left\{ \frac{2s\mu^2 \Sigma_s}{\Sigma_s + s\mu^2} + (\Sigma_s - 2s\mu^2) \ln \frac{\Sigma_s + s\mu^2}{s\mu^2} \right\}, \quad (\text{B4})$$

with $\Sigma_s = (s - (M + m)^2)(s - (M - m)^2) = 4M^2 \vec{k}^2$. The high-energy behavior of the relevant cross sections in the OPE approximation is following:

$$\sigma^{1\gamma}(\omega) \underset{\omega \gg}{\sim} \omega^0, \quad \sigma_{++}^{1\gamma}(\omega) - \sigma_{+-}^{1\gamma}(\omega) \underset{\omega \gg}{\sim} \omega^{-1} \ln \omega, \quad \sigma_{\perp}^{1\gamma}(\omega) - \sigma_{\parallel}^{1\gamma}(\omega) \underset{\omega \gg}{\sim} \omega^{-2} \ln \omega. \quad (\text{B5})$$

The unsubtracted DR for the amplitude $f_+^{2\gamma}$ of Eq. (15) is divergent as ω , therefore we use the subtracted DR of Eq. (18) for this amplitude.

The helicity amplitude corresponding with the TPE direct box graph $T_{h'\lambda'h\lambda}^{2\gamma}$ is given by

$$T_{h'\lambda'h\lambda}^{2\gamma} = \int \frac{e^4 d^4 q}{(2\pi)^4 i} \frac{\bar{u}(k, h') \gamma^\mu (\gamma \cdot (k - q) + m) \gamma^\nu u(k, h) \bar{N}(p, \lambda') \gamma_\mu (\gamma \cdot (p + q) + M) \gamma_\nu N(p, \lambda)}{((p + q)^2 - M^2)((k - q)^2 - m^2)(q^2 - \mu^2)(q^2 - \mu^2)}, \quad (\text{B6})$$

with $\gamma \cdot a \equiv \gamma^\mu a_\mu$. We find the contribution of the direct box graph to the forward amplitudes $f_+^{2\gamma, \text{dir}}$, $f_-^{2\gamma, \text{dir}}$ with exchange of two photons (see Fig. 1) multiplying the fermion spinors by the spin projection operators. Then we sum over all possible polarizations evaluating traces of the Dirac matrices. The direct amplitudes $f_+^{2\gamma, \text{dir}}$, $f_-^{2\gamma, \text{dir}}$ are given by

$$f_+^{2\gamma, \text{dir}} = -8e^4 \frac{\partial}{\partial \mu^2} \int \frac{id^4 q}{(2\pi)^4} \frac{1}{(p + q)^2 - M^2} \frac{1}{(k - q)^2 - m^2} \frac{1}{q^2 - \mu^2} \times (2M^2 \nu_\gamma^2 - q^2 M \nu_\gamma - (p \cdot q)(2M \nu_\gamma + m^2 + (k \cdot q)) + (k \cdot q)(2M \nu_\gamma + M^2)), \quad (\text{B7})$$

$$f_-^{2\gamma, \text{dir}} = 8e^4 \frac{\partial}{\partial \mu^2} \int \frac{id^4 q}{(2\pi)^4} \frac{M}{(p + q)^2 - M^2} \frac{m}{(k - q)^2 - m^2} \frac{1}{q^2 - \mu^2} (q^2 (s \cdot S) - (q \cdot s)(q \cdot S)), \quad (\text{B8})$$

with the lepton and proton spin vectors in the laboratory frame $s = (|\vec{k}|, 0, 0, \omega)/m$ and $S = (0, 0, 0, -1)$. For the double spin-flip amplitude $g^{2\gamma, \text{dir}}$ we use the decomposition in terms of the scalar integrals, since the evaluation of traces can not be exploited here due to the different spin directions of the initial and final fermions. Furthermore, we repeat the same steps for the crossed box graph contribution.

The optical theorem of Eqs. (12, 13), the once-subtracted DR for $f_+^{2\gamma}$ amplitude of Eq. (18), the unsubtracted DRs for $f_-^{2\gamma}$, $g^{2\gamma}$ amplitudes of Eqs. (16, 17) and the amplitudes properties under the crossing $\omega \rightarrow -\omega$ of Eqs. (9-11) were checked comparing with the sum of the direct and crossed box graphs.

Appendix C: Forward invariant amplitudes in terms of the proton structure functions

Substituting expressions for the inclusive cross sections of Eqs. (25-27) into DRs, see Eqs. (15-17), we change the integration order and express the forward TPE amplitudes in terms of the proton SFs:

$$\Re f_+^{2\gamma}(\omega) = 4\alpha^2 M \int_0^\infty \frac{dQ^2}{Q^2} \int_{\nu_{\text{thr}}}^\infty \frac{d\nu_\gamma}{\nu_\gamma} \left\{ \frac{4m^2\nu_\gamma}{MQ^2} (1 - 2\tau_l) I_1^0 F_1(\nu_\gamma, Q^2) + \left(I_1^0 + \frac{4m\nu_\gamma}{Q^2} I_2^0 - \frac{I_3^0}{\tau_l} \right) F_2(\nu_\gamma, Q^2) \right\}, \quad (\text{C1})$$

$$\Re f_-^{2\gamma}(\omega) = 16\alpha^2 \omega \int_0^\infty \frac{dQ^2}{Q^2} \int_{\nu_{\text{thr}}}^\infty \frac{d\nu_\gamma}{\nu_\gamma} \left\{ \left(-I_1^0 + (\tau_l + \tilde{\tau}) I_1^1 + \frac{\nu_\gamma}{m} \left(\frac{I_0^0}{2} + I_0^1 \right) \right) g_1(\nu_\gamma, Q^2) + \frac{Q^2}{2m\nu_\gamma} I_0^0 g_2(\nu_\gamma, Q^2) \right\}, \quad (\text{C2})$$

$$\Re g^{2\gamma}(\omega) = 8\alpha^2 m \int_0^\infty \frac{dQ^2}{Q^2} \int_{\nu_{\text{thr}}}^\infty \frac{d\nu_\gamma}{\nu_\gamma} \left\{ \left(I_1^0 + (\tau_l + \tilde{\tau}) I_1^1 + \frac{\nu_\gamma}{m} (I_0^0 + I_0^1) \right) g_1(\nu_\gamma, Q^2) + 2I_1^0 g_2(\nu_\gamma, Q^2) \right\}, \quad (\text{C3})$$

with the DR master integrals (we introduce the cut-off Λ in the divergent integrals):

$$I_0^0 = \int_{\omega_0}^\infty \frac{-m}{\omega'^2 - \omega^2} \frac{d\omega'}{\sqrt{\omega'^2 - m^2}} = \frac{m}{2|\vec{k}|\omega} \ln \frac{\omega + |\vec{k}|\omega|\vec{k}_0| - |\vec{k}|\omega_0}{\omega - |\vec{k}|\omega|\vec{k}_0| + |\vec{k}|\omega_0}, \quad (\text{C4})$$

$$I_1^0 = \int_{\omega_0}^\infty \frac{-\omega'}{\omega'^2 - \omega^2} \frac{d\omega'}{\sqrt{\omega'^2 - m^2}} = \frac{1}{2|\vec{k}|} \ln \frac{|\vec{k}| - |\vec{k}_0|}{|\vec{k}| + |\vec{k}_0|}, \quad (\text{C5})$$

$$I_2^0 = \frac{1}{m} \int_{\omega_0}^\Lambda \frac{-\omega'^2}{\omega'^2 - \omega^2} \frac{d\omega'}{\sqrt{\omega'^2 - m^2}} = \frac{1}{m} \ln \frac{2\Lambda}{\omega_0 + |\vec{k}_0|} + \frac{\omega}{2m|\vec{k}|} \ln \frac{\omega + |\vec{k}|\omega|\vec{k}_0| - |\vec{k}|\omega_0}{\omega - |\vec{k}|\omega|\vec{k}_0| + |\vec{k}|\omega_0}, \quad (\text{C6})$$

$$I_3^0 = \frac{1}{m^2} \int_{\omega_0}^\Lambda \frac{-\omega'^3}{\omega'^2 - \omega^2} \frac{d\omega'}{\sqrt{\omega'^2 - m^2}} = \frac{|\vec{k}_0| - \Lambda}{m^2} + \frac{\omega^2}{2|\vec{k}|m^2} \ln \frac{|\vec{k}| - |\vec{k}_0|}{|\vec{k}| + |\vec{k}_0|}, \quad (\text{C7})$$

$$I_0^1 = \int_{\omega_0}^\infty \frac{-m^3}{\omega'^2 - \omega^2} \frac{d\omega'}{(\omega'^2 - m^2)^{3/2}} = \frac{\omega_0 m}{|\vec{k}_0|\vec{k}^2} - \frac{m}{\vec{k}^2} + \frac{m^3}{2|\vec{k}|^3\omega} \ln \frac{\omega + |\vec{k}|\omega|\vec{k}_0| - |\vec{k}|\omega_0}{\omega - |\vec{k}|\omega|\vec{k}_0| + |\vec{k}|\omega_0}, \quad (\text{C8})$$

$$I_1^1 = \int_{\omega_0}^{\infty} \frac{-m^2 \omega'}{\omega'^2 - \omega^2} \frac{d\omega'}{(\omega'^2 - m^2)^{3/2}} = \frac{m^2}{\vec{k}^2 |\vec{k}_0|} + \frac{m^2}{2|\vec{k}|^3} \ln \frac{|\vec{k}| - |\vec{k}_0|}{|\vec{k}| + |\vec{k}_0|}. \quad (\text{C9})$$

The reasonable result for the nucleon or narrow Δ contribution, when we are allowed to interchange the ω and Q^2 , ν_γ integration order, is given by the once-subtracted dispersion relation of Eq. (18). It can be obtained from the subtracted at the point ω_s Eq. (C1) by $\Re f_+^{2\gamma}(\omega) - \Re f_+^{2\gamma}(\omega_s)$:

$$\begin{aligned} \Re f_+^{2\gamma}(\omega) - \Re f_+^{2\gamma}(m) &= \frac{4m\alpha^2}{|\vec{k}|} \\ &\times \int_0^\infty \frac{dQ^2}{Q^2} \int_{\nu_{\text{thr}}}^\infty \frac{d\nu_\gamma}{\nu_\gamma} \left(\frac{\nu_\gamma (1 - 2\tau_l)}{2m\tau_l} \left(\ln \frac{|\vec{k}| - |\vec{k}_0|}{|\vec{k}| + |\vec{k}_0|} + \frac{2|\vec{k}|}{|\vec{k}_0|} \right) F_1(\nu_\gamma, Q^2) \right. \\ &+ \frac{2M\nu_\gamma}{mQ^2} \left(\omega \ln \frac{(\omega + |\vec{k}|)^2 (\omega_0^2 - \omega^2)}{(\omega |\vec{k}_0| + |\vec{k}| \omega_0)^2} + 2(\omega_0 - |\vec{k}_0|) \frac{|\vec{k}|}{|\vec{k}_0|} \right) F_2(\nu_\gamma, Q^2) \\ &\left. - \frac{M}{m} \left(\frac{\omega^2 - m^2 \tau_l}{2m^2 \tau_l} \ln \frac{|\vec{k}| - |\vec{k}_0|}{|\vec{k}| + |\vec{k}_0|} + \frac{1 - \tau_l}{\tau_l} \frac{|\vec{k}|}{|\vec{k}_0|} \right) F_2(\nu_\gamma, Q^2) \right). \quad (\text{C10}) \end{aligned}$$

The ν_γ integrals for the spin-dependent amplitudes of Eqs. (32, 33) are convergent.

Due to the Regge behavior of the F_1 proton structure function given by the Pomeron exchange, the ν_γ integrals are divergent, and the DR for the amplitude $f_+^{2\gamma}$ is not applicable for the inelastic intermediate states TPE contribution.

Appendix D: HFS through the forward double virtual Compton scattering amplitudes

It is instructive to evaluate the HFS correction cutting only the lower blob of the TPE graph [42, 43], see right panel in Fig. 10.

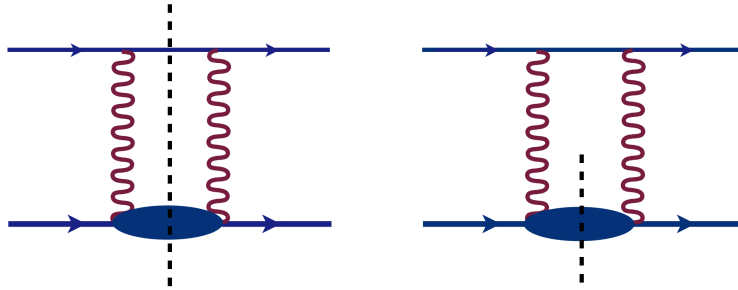


FIG. 10: Forward elastic lp scattering with cut of both fermion lines (left panel) and with cut of the nucleon line only (right panel).

The forward TPE amplitude can be evaluated considering the lower blob of the TPE graph in Fig. 1 as a forward VVCS process on a proton: $\gamma^*(q, \lambda_1) + N(p, \lambda) \rightarrow \gamma^*(q, \lambda_2) + N(p, \lambda')$,

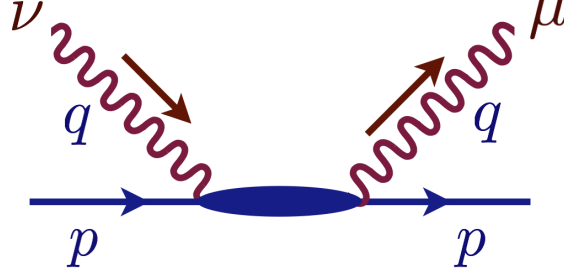


FIG. 11: Forward VVCS process.

which is shown in Fig. 11. The forward VVCS amplitude $T_{\lambda_2\lambda',\lambda_1\lambda}$ can be written in terms of the forward VVCS tensor $M^{\mu\nu}$ as

$$T_{\lambda_2\lambda',\lambda_1\lambda} = \varepsilon_\nu(q, \lambda_1) \varepsilon_\mu^*(q, \lambda_2) \cdot \bar{N}(p, \lambda') (4\pi M^{\mu\nu}) N(p, \lambda), \quad (\text{D1})$$

where $\varepsilon_\nu, \varepsilon_\mu^*$ denote the virtual photon polarization vectors, N, \bar{N} the proton spinors, and $\lambda_1, \lambda_2 (\lambda, \lambda')$ the photon (proton) helicities.

The forward VVCS tensor $M^{\mu\nu}$ can be expressed as the sum of a symmetric (spin-independent) $M_S^{\mu\nu}$ and an antisymmetric (spin-dependent) $M_A^{\mu\nu}$ parts:

$$M^{\mu\nu} = M_S^{\mu\nu} + M_A^{\mu\nu}, \quad (\text{D2})$$

$$M_S^{\mu\nu} = \left(-g^{\mu\nu} + \frac{q^\mu q^\nu}{q^2} \right) T_1(\nu_\gamma, Q^2) + \frac{1}{M^2} \left(p^\mu - \frac{(p \cdot q)}{q^2} q^\mu \right) \left(p^\nu - \frac{(p \cdot q)}{q^2} q^\nu \right) T_2(\nu_\gamma, Q^2), \quad (\text{D3})$$

$$M_A^{\mu\nu} = \frac{1}{2M^2} \left[M\{\gamma^{\mu\nu}, \gamma \cdot q\} S_1(\nu_\gamma, Q^2) + \left([\gamma^\mu, \gamma^\nu] q^2 + q^\mu [\gamma^\nu, \gamma \cdot q] + q^\nu [\gamma \cdot q, \gamma^\mu] \right) S_2(\nu_\gamma, Q^2) \right], \quad (\text{D4})$$

with the forward Compton amplitudes T_1, T_2, S_1, S_2 , which are functions of ν_γ, Q^2 and enter Eq. (D2) in a gauge-invariant way, e.g., $q_\mu M^{\mu\nu} = q_\nu M^{\mu\nu} = 0$. The optical theorem relates the imaginary parts of the forward Compton amplitudes to the proton SFs by

$$\Im T_1(\nu_\gamma, Q^2) = \pi F_1(\nu_\gamma, Q^2), \quad \Im T_2(\nu_\gamma, Q^2) = \frac{\pi M}{\nu_\gamma} F_2(\nu_\gamma, Q^2), \quad (\text{D5})$$

$$\Im S_1(\nu_\gamma, Q^2) = \frac{\pi M}{\nu_\gamma} g_1(\nu_\gamma, Q^2), \quad \Im S_2(\nu_\gamma, Q^2) = \frac{\pi M^2}{\nu_\gamma^2} g_2(\nu_\gamma, Q^2). \quad (\text{D6})$$

The forward lepton-proton scattering TPE amplitude can be expressed in terms of the forward VVCS amplitude $M^{\mu\nu}$ as

$$T_{h'\lambda'h\lambda}^{2\gamma}(\omega) = e^2 \int \frac{id^4q}{(2\pi)^3} \frac{\tilde{L}_{h'h}^{\mu\nu} \bar{N}(p, \lambda') M_{\mu\nu} N(p, \lambda)}{(q^2)^2}, \quad (\text{D7})$$

with the leptonic tensor $\tilde{L}_{h'h}^{\mu\nu}$:

$$\tilde{L}_{h'h}^{\mu\nu} = \bar{u}(k, h') \left(\gamma^\mu \frac{\hat{k} - \hat{q} + m}{(k - q)^2 - m^2} \gamma^\nu + \gamma^\nu \frac{\hat{k} + \hat{q} + m}{(k + q)^2 - m^2} \gamma^\mu \right) u(k, h). \quad (\text{D8})$$

The expression for the spin-independent forward TPE amplitude $f_+^{2\gamma}$ is given by

$$f_+^{2\gamma}(\omega) = -4e^4 \int \frac{id^4q}{(2\pi)^4} \frac{(k \cdot q)^2 (2T_1 - T_2) + q^2 (m^2 T_1 - \omega^2 T_2) + \frac{2\omega}{M} (k \cdot q) (p \cdot q) T_2}{(q^4 - 4(k \cdot q)^2) (q^2)^2}. \quad (D9)$$

This result at threshold is in agreement with Ref. [25].

The expressions for the spin-dependent forward TPE amplitudes $f_-^{2\gamma}$, $g^{2\gamma}$ are given by

$$f_-^{2\gamma}(\omega) = -\frac{8\alpha}{M^3} \int \frac{id^4q}{\pi^2} \frac{\left(M^2 q^2 + \frac{M^2(k \cdot q)^2 + m^2(p \cdot q)^2 - 2(k \cdot p)(k \cdot q)(p \cdot q)}{\omega^2 - m^2} \right) (k \cdot p) S_1 + M^2 q^2 (k \cdot q) S_2}{(q^4 - 4(k \cdot q)^2) q^2} - \frac{8\alpha}{M} \int \frac{id^4q}{\pi^2} \frac{(k \cdot q) (p \cdot q) S_1}{(q^4 - 4(k \cdot q)^2) q^2}, \quad (D10)$$

$$g^{2\gamma}(\omega) = \frac{4m\alpha}{M^2} \int \frac{id^4q}{\pi^2} \frac{\left(M^2 q^2 - \frac{M^2(k \cdot q)^2 + m^2(p \cdot q)^2 - 2(k \cdot p)(k \cdot q)(p \cdot q)}{\omega^2 - m^2} \right) S_1 + 2q^2 (p \cdot q) S_2}{(q^4 - 4(k \cdot q)^2) q^2}. \quad (D11)$$

Evaluating these expressions in the nucleon rest frame at threshold we obtain:

$$g^{2\gamma}(m) = -f_-^{2\gamma}(m) = \frac{8m}{M^2} e^4 \int \frac{id^4q}{(2\pi)^4} \frac{q^2 \nu_\gamma S_2 + M \frac{2q^2 + \nu_\gamma^2}{3} S_1}{(q^4 - 4(k \cdot q)^2) q^2}, \quad (D12)$$

in agreement with Eq. (40) and the standard HFS derivation of Eq. (47) [35–40].

Exploiting DRs for the spin-dependent Compton amplitudes S_1 and S_2 :

$$\Re S_1(\nu_\gamma, Q^2) = \int_{\nu_{\text{thr}}}^{\infty} \frac{2M g_1(\nu'_\gamma, Q^2)}{\nu_\gamma'^2 - \nu_\gamma^2 - i\varepsilon} d\nu'_\gamma, \quad (D13)$$

$$\Re S_2(\nu_\gamma, Q^2) = \int_{\nu_{\text{thr}}}^{\infty} \frac{2\nu_\gamma M^2 g_2(\nu'_\gamma, Q^2)}{\nu_\gamma'^2 (\nu_\gamma'^2 - \nu_\gamma^2 - i\varepsilon)} d\nu'_\gamma, \quad (D14)$$

we obtain the same expression for the amplitude $f_-^{2\gamma}$, see Eq. (37), as with the DRs for the forward lp amplitudes. The difference in the amplitude $g^{2\gamma}$, see Eq. (38), is given by the ω -independent term, which is just the constant real part in $g^{2\gamma}$ amplitude. It vanishes with account of the BC sum rule. However, if one uses the DR for the amplitude $\nu_\gamma S_2$ [49], the result for $f_-^{2\gamma}(m)$ coincides with the expression $-g^{2\gamma}(m)$.

The forward TPE amplitudes evaluated within the DR approach coincide with the amplitudes evaluated with a help of the DRs for the forward VVCS amplitudes. However, the contribution of an individual TPE intermediate state differs in these two approaches.

Appendix E: Forward scattering observables

The forward unpolarized elastic scattering cross section in the c.m. reference frame is given by

$$\frac{d\sigma}{d\Omega}(\theta = 0) = \frac{|f_+(\omega)|^2 + |f_-(\omega)|^2 + 2|g(\omega)|^2}{64\pi^2(M^2 + 2M\omega + m^2)}, \quad (E1)$$

with the electron scattering angles Ω and the azimuthal angle θ .

All possible single-spin asymmetries are zero for the scattering in the forward direction. We denote the lepton spin asymmetry for the scattering on the polarized proton as A and for the scattering on the unpolarized proton with the polarization transfer to the final proton as P . The asymmetries for the longitudinally polarized lepton and the longitudinally polarized proton in the forward scattering are expressed as

$$A_l = \frac{d\sigma_{+-} - d\sigma_{--}}{d\sigma_{+-} + d\sigma_{--}} = -2 \frac{\Re(f_+ f_-^*) + |g|^2}{|f_+|^2 + |f_-|^2 + 2|g|^2}, \quad (\text{E2})$$

$$P_l = \frac{d\sigma_{+-} - d\sigma_{--}}{d\sigma_{+-} + d\sigma_{--}} = -2 \frac{\Re(f_+ f_-^*) - |g|^2}{|f_+|^2 + |f_-|^2 + 2|g|^2}. \quad (\text{E3})$$

The asymmetries for the transversely polarized lepton and the transversely polarized proton in the forward scattering are expressed as

$$A_t = \frac{d\sigma_{\uparrow\uparrow} - d\sigma_{\uparrow\downarrow}}{d\sigma_{\uparrow\uparrow} + d\sigma_{\uparrow\downarrow}} = 2 \frac{\Re((f_+ + f_-) g^*)}{|f_+|^2 + |f_-|^2 + 2|g|^2}, \quad (\text{E4})$$

$$P_t = \frac{d\sigma_{\uparrow\uparrow} - d\sigma_{\uparrow\downarrow}}{d\sigma_{\uparrow\uparrow} + d\sigma_{\uparrow\downarrow}} = 2 \frac{\Re((f_+ - f_-) g^*)}{|f_+|^2 + |f_-|^2 + 2|g|^2}. \quad (\text{E5})$$

The asymmetries in the case of one transverse and one longitudinal polarizations vanish.

-
- [1] M. N. Rosenbluth, Phys. Rev. **79**, 615 (1950).
 - [2] M. K. Jones *et al.* [Jefferson Lab Hall A Collaboration], Phys. Rev. Lett. **84**, 1398 (2000).
 - [3] P. A. M. Guichon and M. Vanderhaeghen, Phys. Rev. Lett. **91**, 142303 (2003).
 - [4] P. G. Blunden, W. Melnitchouk and J. A. Tjon, Phys. Rev. Lett. **91**, 142304 (2003).
 - [5] C. E. Carlson and M. Vanderhaeghen, Ann. Rev. Nucl. Part. Sci. **57**, 171 (2007).
 - [6] J. Arrington, P. G. Blunden and W. Melnitchouk, Prog. Part. Nucl. Phys. **66**, 782 (2011).
 - [7] I. A. Rachek *et al.*, Phys. Rev. Lett. **114**, no. 6, 062005 (2015).
 - [8] B. S. Henderson *et al.*, arXiv:1611.04685 [nucl-ex].
 - [9] D. Adikaram *et al.* [CLAS Collaboration], Phys. Rev. Lett. **114**, 062003 (2015).
 - [10] R. Pohl *et al.*, Nature **466**, 213 (2010).
 - [11] A. Antognini *et al.*, Science **339**, 417 (2013).
 - [12] J. C. Bernauer *et al.* [A1 Collaboration], Phys. Rev. Lett. **105**, 242001 (2010).
 - [13] J. C. Bernauer *et al.* [A1 Collaboration], Phys. Rev. C **90**, no. 1, 015206 (2014).
 - [14] P. J. Mohr, B. N. Taylor and D. B. Newell, Rev. Mod. Phys. **84**, 1527 (2012).
 - [15] C. E. Carlson, Prog. Part. Nucl. Phys. **82**, 59 (2015).
 - [16] R. Pohl [CREMA Collaboration], J. Phys. Soc. Jap. **85**, no. 9, 091003 (2016).
 - [17] A. Dupays, A. Beswick, B. Lepetit, C. Rizzo and D. Bakalov, Phys. Rev. A **68**, 052503 (2003).
 - [18] Y. Ma *et al.*, Int. J. Mod. Phys. Conf. Ser. **40**, 1660046 (2016).
 - [19] A. Adamczak *et al.* [FAMU Collaboration], JINST **11**, no. 05, P05007 (2016).
 - [20] K. Pachucki, Phys. Rev. A **53**, 2092 (1996).
 - [21] R. N. Faustov and A. P. Martynenko, Phys. Atom. Nucl. **63**, 845 (2000).
 - [22] A. Pineda, Phys. Rev. C **67**, 025201 (2003).
 - [23] A. Pineda, Phys. Rev. C **71**, 065205 (2005).
 - [24] D. Nevado and A. Pineda, Phys. Rev. C **77**, 035202 (2008).
 - [25] C. E. Carlson and M. Vanderhaeghen, Phys. Rev. A **84**, 020102 (2011).
 - [26] M. C. Birse and J. A. McGovern, Eur. Phys. J. A **48**, 120 (2012).
 - [27] J. M. Alarcon, V. Lensky and V. Pascalutsa, Eur. Phys. J. C **74**, no. 4, 2852 (2014).
 - [28] C. Peset and A. Pineda, Nucl. Phys. B **887**, 69 (2014).
 - [29] R. J. Hill, G. Lee, G. Paz and M. P. Solon, Phys. Rev. D **87**, 053017 (2013).
 - [30] R. J. Hill and G. Paz, arXiv:1611.09917 [hep-ph].
 - [31] M. Gorchtein, F. J. Llanes-Estrada and A. P. Szczepaniak, Phys. Rev. A **87**, no. 5, 052501 (2013).
 - [32] O. Tomalak and M. Vanderhaeghen, Eur. Phys. J. C **76**, no. 3, 125 (2016).
 - [33] I. Caprini, Phys. Rev. D **93**, no. 7, 076002 (2016).
 - [34] A. C. Zemach, Phys. Rev. **104**, 1771 (1956).
 - [35] C. K. Iddings and P. M. Platzman, Phys. Rev. **113**, 192 (1959).
 - [36] C. K. Iddings, Phys. Rev. **138**, B446 (1965).
 - [37] S. D. Drell and J. D. Sullivan, Phys. Rev. **154**, 1477 (1967).
 - [38] R. N. Faustov, Nucl. Phys. **75**, 669 (1966).
 - [39] G. M. Zinovjev, B. V. Struminski, R. N. Faustov, and V. L. Chernyak, Sov. J. Nucl. Phys. **11**, 715 (1970).
 - [40] G. T. Bodwin and D. R. Yennie, Phys. Rev. D **37**, 498 (1988).
 - [41] R. N. Faustov, E. V. Cherednikova and A. P. Martynenko, Nucl. Phys. A **703**, 365 (2002).

- [42] C. E. Carlson, V. Nazaryan and K. Griffioen, Phys. Rev. A **78**, 022517 (2008).
- [43] C. E. Carlson, V. Nazaryan and K. Griffioen, Phys. Rev. A **83**, 042509 (2011).
- [44] A. Denig and H. Merkel, Talk at New Vistas in Low-Energy Precision Physics, Mainz, Germany, 2016.
- [45] X. Zheng [CLAS/EG4 Collaboration], AIP Conf. Proc. **1155**, 135 (2009).
- [46] S. Choi [SANE Collaboration], AIP Conf. Proc. **1388**, 480 (2011).
- [47] A. Camsonne, J. P. Chen, D. Crabb and K. Slifer, JLab E08-027 (g2p) experiment.
- [48] C. Peset and A. Pineda, arXiv:1612.05206 [nucl-th].
- [49] F. Hagelstein, R. Miskimen and V. Pascalutsa, Prog. Part. Nucl. Phys. **88**, 29 (2016).
- [50] M. Gell-Mann, M. L. Goldberger and W. E. Thirring, Phys. Rev. **95**, 1612 (1954).
- [51] V. Pascalutsa and M. Vanderhaeghen, Phys. Rev. Lett. **105**, 201603 (2010).
- [52] W. Grein and P. Kroll, Nucl. Phys. B **137**, 173 (1978).
- [53] P. Kroll, Lett. Nuovo Cim. **7**, 745 (1973).
- [54] P. A. M. Guichon, Nucl. Phys. A **402**, 541 (1983).
- [55] M. Gorchtein, Phys. Lett. B **644**, 322 (2007).
- [56] D. Borisjuk and A. Kobushkin, Phys. Rev. C **78**, 025208 (2008).
- [57] O. Tomalak. 2016. Dissertation, Johannes Gutenberg-Universität Mainz.
- [58] G. A. Miller, Phys. Lett. B **718**, 1078 (2013).
- [59] L. C. Maximon and J. A. Tjon, Phys. Rev. C **62**, 054320 (2000).
- [60] K. A. Olive *et al.* [Particle Data Group Collaboration], Chin. Phys. C **38**, 090001 (2014).
- [61] J. Blumlein and N. Kochelev, Nucl. Phys. B **498**, 285 (1997).
- [62] S. E. Kuhn, J.-P. Chen and E. Leader, Prog. Part. Nucl. Phys. **63**, 1 (2009).
- [63] K. A. Griffioen, S. Kuhn, N. Guler, personal communication, 2015.
- [64] N. Sato *et al.* [Jefferson Lab Angular Momentum Collaboration], Phys. Rev. D **93**, no. 7, 074005 (2016).
- [65] Y. Prok *et al.* [CLAS Collaboration], Phys. Lett. B **672**, 12 (2009).
- [66] D. Drechsel, S. S. Kamalov and L. Tiator, Phys. Rev. D **63**, 114010 (2001).
- [67] D. Drechsel, S. S. Kamalov and L. Tiator, Eur. Phys. J. A **34**, 69 (2007).
- [68] D. Drechsel, B. Pasquini and M. Vanderhaeghen, Phys. Rept. **378**, 99 (2003).
- [69] V. Pascalutsa and M. Vanderhaeghen, Phys. Rev. D **91**, 051503 (2015).
- [70] V. Lensky, V. Pascalutsa, M. Vanderhaeghen and C. Kao, arXiv:1701.01947 [hep-ph].